Emerging Trends in Engineering and Technology

Volume - 2

Chief Editor

Mohit Bajpai

Associate Professor, Electronics and Communication Engineering, Poornima Institute of Engineering & Technology, Jaipur, Rajasthan, India

Co-Editor

Dr. A.V. Sudhakara Reddy

Associate Professor, R&D Coordinator, Department of Electrical and Electronics Engineering, Malla Reddy Engineering College (Autonomous), Maisammaguda, Secunderabad, Telangana, India

Integrated Publications
New Delhi

Published By: Integrated Publications

Integrated Publications
H. No. - 3 Pocket - H34, Sector - 3,
Rohini, Delhi-110085, India

Chief Editor: Mohit Bajpai

Publication Year: 2021

Pages: 108

ISBN: 978-93-90471-14-0

Book DOI: https://doi.org/10.22271/int.book.72

Price: ₹ 718/-

Contents

Chapter - 1
E-Waste: Formation and Their Consequences

Author

Simanchal Dash
Department of Chemistry, Roland Institute of Technology,
Berhampur, Odisha, India

Chapter - 1

E-Waste: Formation and Their Consequences

Simanchal Dash

Abstract

An electronic and electrical product which is no more use and discarded or recycled is known as electronic waste or e-waste. Constantly rise of handling in electronics and electrical equipments has produced a large no of e-waste. At present in India practices of e-waste management encounters many challenges. Out of them some of the most significant are insufficient awareness in consumers, problem in informal cycling, difficulty in inventorization and improper regulations. Adverse impact on the environment and human health consequences rises by entering toxic materials into the waste stream. The vast creation of e-waste has formed a new e-waste stream in the country containing no more used goods, fulfilled life of electrical and electronics goods after their requisite use. Different factors like innovation, product design and globalization replace these equipments in very little span of time and made it speedy by rising waste in the earth. The e-waste treatment infrastructure is limited in India and casual recycling continues to exist under the domain of flexible legislative frame. The waste managing agencies in our country is more pertaining to the presence of toxic and hazardous substances in e-wasted equipments on account of their effect on human health and environment. The survival and execution of environmentally sound management is limited and moving ahead very slowly due to apparent reasons. The formal recyclers have specially made wide-ranging e-waste treatment methods but not according to the e-waste generated in the country at the same time the informal recyclers are treating most of the e-waste produced with hazardous ways.

Keywords: e-waste, environment, recycling, globalization, toxic and hazardous substances

1. Introduction

In today's information age, the whole society is linked, informed and connected in appropriate manner and made a significant technological

advance in electronics and information science boosting the economy and enhancing the lifestyle of a common man. The whole dependence on electronic products has paved the way for an emerging environmental concern over electronic waste. The waste generated from used electronic devices as well as household appliances and those are not fit for their further use and are intended for recovery, recycling or disposal is known as E-waste. It usually consists of wide range of electrical and electronic devices like computers, mobile phones, sound boxes as well as different parts of refrigerators, air conditioners etc. E-waste holds nearly one thousand various substances having toxic and hazardous nature. There is a remarkable growth in the manufacturing and consumption of electronic and electrical equipment in the recent years due to human requirement. As per the statement given by Economic Cooperation and Development (OECD) any device using in domestic and electronic with the help of electronic power supply that has exhausted its complete life is known as waste from electronic and electrical equipments (WEEE). WEEE is a term which has received maximum attention over past 15 years. Almost 90% of the total waste generation belongs three categories of WEEE which includes house hold appliances of 42% which is first followed by ICT equipment with 34% and consumer electronics having 14% [1]. During the time period of 1994 to 2007 desktop selling is maximum value of 5.52 million [2]. At the same time the mobile subscriber in India changes from 90 million to 433 million during the period 2006-11 and attained 900 million in 2015-16 [3-4]. On account of increasing demand of information technology and its application in the society computer waste is growing very much as compared to other e-waste. As a result of this, quick product obsolescence multiplied with lower costs discarded electronic and electrical equipment results in the high alarming waste problem in the world. Different companies today design their products for planned obsolescence. This creates toughness by marketing and retailing practices with affordable and convenience that have been taken over from product durability as key drivers [5]. It is a significant matter that the generated E-waste contains both toxic and valuable materials inside it. The metals like iron, copper, aluminum, gold and other in a E-waste is nearly 60% where as the pollutants comprises of 2.70% [6]. Hence recycling of E-waste is important with regard to the point of waste treatment and also from the recovery of expensive materials. It has been estimated that nearly 100 million computers and other electronic devices break or become no more use every year. Many of these products can be reused, refurbished or recycled. Management of E-waste is very critical task because it contains toxic materials and there is a large number of computers, televisions, mobile phones and other electronic products that are disposed every year contains

such toxic substances. When these substances is dumped in landfills or when the waste is incinerated then various contaminants and toxic chemicals are formed and evolved into the ground making pollution of the environment. At the same time E-waste being produced at an alarming rate due to fast obsolescence along with speedily evolving technology. The process of E-waste disposal is very complex because of its involvement with many people, enterprises, extensive areas and long-time span.

2. Constituents of e-waste

Waste from Electronic and Electrical equipment (WEEE) consist of a number of components with some toxic substances. Unless and otherwise toxic substances treated properly can affect human health and environment. Normally, these hazards occur due to improper recycling and disposal methods chosen. There are number of harmful metals found in e-waste. Some of them are discussed here.

i) Antimony

Some of the main uses of antimony are alloys, electronics flame proofing, ceramics, rubber and paints. When antimony forms alloy with lead it provides hardness and strength. Basically it is used as a hardener in lead storage batteries. Health problems like headaches, dizziness and depression are developed with small doses of antimony while larger doses can causes vomiting.

ii) Arsenic

It is found in light emitting diodes in the form of gallium arsenide in little quantity. It is a poisonous metallic element and long contact with it can lead to skin diseases and lung cancer.

iii) Aluminum

It is present in more or less in all electronic products. It also provides conductivity. Its more utility is on account of it’s less cost in comparison to gold and silver. It can be easily recyclable.

iv) Barium

It is a metallic element used in sparkplugs, fluorescent lamps and in vacuum tubes. It creates poisonous oxides while come in contact with air. Barium causes muscle weakness, liver and heart problems. This metal is found in computers front panel of CRT and it used to protect users from radiation. Brain swelling, muscle weakness, damage to the heart and liver are formed with short-term exposure to barium.

v) Brominated Flame Retardants (BFRs)

In order to prevent flammability, it is used in the plastic housings of electronic equipment and in circuit boards. More than half of BFR usage in the electronics industry contains of tetrabromo-bisphenol-(TBBPA), 10% is polybrominated diphenyl ethers (PBDEs) and less than 1% is polybrominated biphenyls (PBB).

vi) Beryllium

Motherboards and finger clips found to be contains beryllium. To strengthen connectors and tiny plugs with maintaining electrical conductivity copper-beryllium alloy is used. Lung cancer can be developed on long exposure to it. It also causes a skin disease that is characterized by poor wound healing and wart like bumps. Beryllium disease are found to be developed after many years of long exposure.

vii) Cadmium

It is present in rechargeable Ni-Cd batteries, CRT screens, printer inks toners, infra-red detectors and semiconductor chips. Kidneys are affected significantly with cadmium components absorbed through respiration. Cadmium containing material increases the pollution to substantial extent due to its toxicity. If it is present large amount in the atmosphere in ionic form then it is directly absorbed in human body. Cadmium oxides and carbonates are the non-toxic in nature. The pollution due to cadmium can be prevented by oxidation with manganese oxide as catalyst.

viii) Chromium

It is found in data tapes and floppy disks. Its highly usefulness due to account of high conductivity and anti-corrosive properties. Irritation of eyes, skin and mucous membranes has to be performed by Chromium (VI) compounds in addition to creating DNA damage.

ix) Gold

It is used in little extent in connectors and PWBs. It is used for providing conductivity and connectivity. Gold has no harmful effects on environment and humans. After all recycling process the metal can be recovered.

x) Copper

It is found on PCB’s, on the internal circuit of keyboard, on the cables and connectors, on IC’s of motherboard, on RAM chip. It is one of the costly materials and can be further used.

xi) Lead

It is found in CRT screens, batteries and printed circuit boards. It is also used in solder, lead acid batteries, electronic components and cable sheathing. Glass panels and gaskets in computer monitors also contains lead. Exposure to high amount of lead can result in vomiting, diarrhea, appetite loss, abdominal pain, constipation, fatigue and sleeplessness. It causes damage to the central and peripheral nervous systems, blood systems, kidney and reproductive system in humans. It also affects the endocrine system and impedes brain development among children. Accumulation of lead in the environment and its high acute and chronic effects on plants, animals and microorganisms.

xii) Mercury

It is used extensively in fluorescent lamps, LCDs, alkaline batteries and mercury wetted switches. Mercury has been used by thermostats, mobile phones, switches, medical equipment and batteries. It is also used in flat panel displays. It is a toxic metal that on bioaccumulation causes brain and liver damage if inhaled. Mercury has a high affinity to accumulate in the body organs in any form. Spreading of inorganic mercury in water leads to formation of methylated mercury which bio-accumulates in living organisms and concentrates through the food chain in the way of fish medium. Methyl mercury are highly toxic in nature. Mercury easily forms nitrates and chlorides which are ionic in nature. In ionic state also mercury is absorbed by human body but ionic mercury can be excreted by kidneys and other organs thus lowering the toxicity level. Mercury causes damage to organs including the brain and kidneys as well as the fetus. The developing fetus is highly vulnerable to mercury exposure.

xiii) Polyvinyl chloride (PVC)

It is an extensively used plastic and electronic appliances. PVC is harmful since it contains about 55% chlorine which when burned gives rise to hydrogen chloride gas. This combines with water to produce hydrochloric acid and if it inhaled can lead to respiratory problems.

xiv) Silver

It is used mainly in connectors and PWBs to provide conductivity. It is typically used in the electronics and keypad contacts in the elemental form.

3. Disposal of e-waste

The produced e-waste can be either recycled and reused or disposed off in landfills or burn in incinerators. The minimization of the hazardous effects

of e-waste can be done by reusing and recycling of outdated electronic products. It helps to also boost energy and resource conservation. At the end when the computer is no more use it has been exhausted and a computer is slated for disposal is sent for recycling. It indicates that the old raw materials are reclaimed for use in making new products. As the cost of recycling is very high hence most recyclers are not very much willing to take computers for recycling. If the waste cannot be even recycled then it have to landfills or is burnt in incinerators. The ground water and soil contaminated due to dumping of waste in to landfills. Toxic chemicals in electronics products leach into the land in course of time and further move into the atmosphere. These toxic substances can migrate into ground waters and finally into lakes, streams, or wells and creates a problem by entering the food chain. Burning electronic products into incinerators releases toxic gases due to the presence of heavy metals such as lead, cadmium and mercury. The food chain bioaccumulated by released mercury into the atmosphere through the fish which is the major route of exposure for the humans. Burning of e-waste creates Brominated flame retardants that generates brominated dioxins and furans. If incineration process is not done perfectly then the plastics and other hydrocarbons not completely oxidized to carbon dioxide with water and they combine with halogens to form new halogenated hydrocarbons including dioxins. Due to advancement of technology lifespan of computers are nearly three to four years and the user instead of changing parts replaces complete system. The toxic substances present in computers are very hazardous for health and environment. Hence, it is unsafe to either burn or landfill the e-waste on account of polluting environment. As e-waste has a serious problem. So it has to be recycled or reused or disposed off. Recycling can be performed in a number of ways like assembling, developing, promoting or buying of new products which are prepared from waste materials. At the same time some toxic substances cannot be recycled on account of its effects on the human health and environment. Burning the e-waste leads into to creation of harmful gases on account of hazardous substances presence. On the other hand if harmful substances can be disposed off with some chemicals then it will lessen the pollution of environment and human health endangered.

4. Environmental impacts of e-waste

4.1 Potential environmental problems related to e-waste

The constituent present in e-wastes depends on the type and the age of the electronic object discarded. Generally it can be determined by several metal alloys like Cu, Al and Fe attached or mixed with some several plastics

or ceramics. Some of the substances like heavy metals are used for the production of electronic items while some others like Polycyclic Aromatic Hydrocarbons (PAHs) are produced by e-waste burning at low temperature. It has been found that burning the isolating plastic cover of cables in open barrels turn out hundred times more dioxins as that of domestic waste [7]. Taking into consideration that the annual e-waste production nearly 20Mt, the total quantities of the several pollutants contained in the e-waste in a maximum extent with respect to landfills or recycling centre's affects the environment and public health. In spite of this, considerable recycling, e-waste is accountable for 5000 t Cu yearly released to the environment [8]. PBDEs (Poly brominated diphenyl ethers) are combustion retardants that to the end results in the environment and forming lipophilic compounds are bioaccumulated in living organisms [9]. Similarly the refrigerators and air-conditioners discarded contain CFCs (Chlorofluorocarbons) that will in the long run annihilate the ozone layer when, in the future, CFCs escape from the e-waste dumping site [10]. The above-mentioned problems raise bigger issue considering the fact that the majority of e-waste are not recycled because of several electronic and electrical items are unnecessary along with household waste and are subject to no further treatment [11]. Something like 80% of the quantity collected for recycling is exported to countries such as Malaysia, Nigeria, Ghana, China, Pakistan, Vietnam, Philippines, etc. [12]. This results in their treatment in very loose environmental frameworks having increased impact on the environment and the employees in the specific operations.

4.2 Environmental pollution caused by e-waste disposal and recycling

The common way of treating e-waste is to landfill sites. The execution of the appropriate way is TCLP (Toxicity Characteristic Leaching Procedure) test has demonstrated that e-waste not needed at urban waste dumping sites do not produce leachates with heavy metals concentrations beyond the environmental limits [13]. On the other hand, this chemical cocktail produced as leachate following the TCLP test from several electronic items was toxic for aquatic organisms [14]. Besides, the usual management practice of e-waste compression discarding in landfills may increase the leachate volumes before or during due to the disturbance of the several electronic circuit parts. For the sake of the reason, it is proposed to perform cement solidification on e-waste that increases pH and decreases the aqueous solutions flow in the waste discarded [15]. Since e-waste recycling comprises disassembling and destroying the individual parts to retrieve several materials. Through the process of recycling of a computer's useful

materials of 95% and of a cathode ray tube's materials of 45% can be retrieved [11]. Least environmental impact can be observed when combined with the application of appropriate technology as used in Japanese recycling methods [16]. But, on the other hand when using the practices followed in developing countries like child labour, e-waste burning and emission of several pollutants to the air, etc. the final environmental benefit impact balance is not always helpful manner. It should be remembered that any environmental benefit from recycling become extinct when the waste to be recycled is transported to large distance on the cost of the adverse environmental impact of the energy consumed for its transportation [17]. At the end, it can be notified that recycling has smaller ecological foot print than e-waste dumping and burning [18].

4.3 Environmental pollution caused by plastics in e-waste obtained from computer

Recycling of WEEE is an important subject in terms of waste treatment and recovery of valuable waste. Although mechanical processing provides a way for recovering valuable materials but some difficulties remains with it. The important one is industries have to afford the taking apart of the different material in WEEE. This problem leads to some approaches to optimize the process. The best way of separation is based on the physical chemical properties of materials to making recycling of material with WEEE economically profitable [19-20]. As per the research finding most of the waste comes from computer bodies and computer monitors. It has been observed that 500 million PCs contain roughly 2,872,000 t of plastics, 718,000 t of lead, 1363 t of cadmium and 287 t of mercury [21]. They also possess 861 t of hexavalent chromium [22]. E-plastics forms nearly 15-22% of the weight of WEEE out of which one third is fit for mechanical recycling and two third needs to dispose by other means [23]. In wealthier countries, e-waste will stand for 8% of the urban waste volume [24]. Electronic computers with an average 3-year life cycle contribute to a greater extent to the total e-waste flow compared to refrigerators and electrical cook-stoves having an average life cycle of 10-12 years [25]. The recycling of this plastic waste generally involves low level of processing such as granulation or pelletization followed by melt or partial melt and extrusion to form the end product. Recycling of plastic waste is difficult because of polymeric materials present there. Thermoplastics and thermosets somewhat high levels of flame retardants added during production. When we try to pick up the plastic material from unnecessary electronic devices, we have to remember that the usual high halogen contents results from the addition of flame retardants. Thermo set polymer cannot be remolded or reprocessed by remelting.

Thermo set composite contain high amount of inorganic glass reinforcement or mineral filler. Fire retardants are often used with plastic material to check the fire safety when create toxic substance during combustion. The smallness of electronic equipment decreases the volume of waste making repairing and recycling a difficult process.

5. Conclusion

Management of E-waste in India is a very difficult task as compared to that of other countries. Of course, there are several problems like the complexity of the E-waste issue in India, vast diversity in its geographical and cultural arena, economic inequalities etc. The most significant thing is rapidly growing E-waste volumes in terms of both domestic and also through imports. Imports are done by second-hand computer donations towards bridging the digital divide. There is a Lack of exact data's of the quantity of E-waste generated and recycled. Some of the factors like insufficient awareness among the manufacturers and consumers of the hazards, incorrect E-waste disposal, recycling of e-waste in the informal sector using rudimentary techniques Like acid treatment methods are the causes for increasing e-waste. E-waste workers have poor idea regarding toxins in E-waste and its exposing causes to serious health hazards. Improper recycling processes make sufficient substantial loss of materials. The main drawback in India there is no such technology or policy to check the disposal of e-waste among the fastest growing waste in the world. There must be consciousness among the users and manufacturer of electronic products.

References

1. Violet NP. E-waste hazard: The impending challenge, Indian J Occup Environ Med. 2008; 12(2):65-70.
2. Dwivedy M, Mittal RK. Future trends in computer waste generation in India, Waste Management. 2010; 30:2265-2277.
3. Singh SK. The diffusion of mobile phones in India, Telecommunications Policy. 2008; 32:642-651.
4. Kumar R, Tripathi S. Electronics-Hi-Tech-Highly Toxic India, Green Peace, 2007.
5. Jennifer C. Distancing the waste: Overconsumption in a global economy, 2005. Retrieved September 30, 2014, from htt://www.learningace.com.
6. Widmer R, Heidi OK, Deepali SM, Heimz B. Global perspective on e-waste'. Environ. Impact Assess. 2005; 25:436.

7. Gullett BK, Linak WP, Touati A, Wasson SJ, Gatica S, King CJ. Characterization of air emissions and residual ash from open burning of electronic wastes during simulated rudimentary recycling operations, J Mater Cycl Waste Manag. 2007; 9:69-79.

8. Bertram M, Graedel TE, Rechberger H, Spatari S. The contemporary European copper cycle: waste management subsystem, Ecol Econ. 2002; 42:43-57.

9. Deng WJ, Zheng JS, Bi XH, Fu JM, Wong MH. Distribution of PBDEs in air particles from an electronic waste recycling site compared with Guangzhou and Hong Kong, South China, Environ Int. 2007; 33:1063-1069.

10. Scheutz C, Mosbaek H, Kjeldsen P. Attenuation of methane and volatile organic compounds in landfill soil covers, J Environ Qual. 2004; 33:61-71.

11. Ladou J, Lovegrove S. Export of electronics equipment waste, Int J Occup Environ Health. 2008; 14:1-10.

12. Schmidt CW, Unfair trade-E-waste in Africa, Environ Health Perspect. 2006; 114:A232-A235.

13. Spalvins E, Dubey B, Townsend T. Impact of electronic waste disposal on lead concentrations in landfill leachate, Environ Sci Technol. 2008; 42:7452-7458.

14. Dagan R, Dubey B, Bitton G, Townsend T. Aquatic toxicity of leachates generated from electronic devices, Arch Environ Contam Toxicol. 2007; 53:168-173.

15. Niu XJ, Li YD. Treatment of waste printed wire boards in electronic waste for safe disposal, J Hazard Mater. 2007; 145:410-416.

16. Aizawa H, Yoshida H, Sakai SI. Current results and future perspectives for Japanese recycling of home electrical appliances, Res Conserv Recycl. 2008; 52:1399-1410.

17. Barba-Gutierrez Y, Adenso-Diaz B, Hopp M. An analysis of some environmental consequences of European electrical and electronic waste regulation, Res Conserv Recycl. 2008; 52:481-495.

18. Hischier R, Wäger P, Gauglhofer J. Does WEEE Recycling make sense from an environmental perspective*?* Environ Impact Assess Rev. 2005; 25:525-539.

19. Shen H, Forssberg E, Pugh RJ. Selective floatation separation of plastics by particle control. Resource Conserve Recycling. 2001; 33:37-50.

20. Pappa G, Boukouvalas C, Giannaris C, Ntaras N, Zografos V, Magoulas K *et al*. The selective dissolution, precipitation technique for polymer recycling a pilot unit application. Resource conserve recycling. 2001; 34:33-44.

21. Puckett J, Smith T. Exporting harm: the high-tech trashing of Asia, The Basel Action Network, Silicon Valley Toxics Coalition, San Jose, Seattle, 2002.

22. SVTC, Take it back! Make it Clean! Make it Green! Computer Take-back Campaign. Silicon Valley Toxics Coalition (SVTC), 2002. Retrieved from: http://www.svtc.org/cleancc/pubs/2002report.

23. Cornelia V. Feed stock recyclic from pplastic and thermoset fractions of used computers (1) pyrolysis. J Mater. cycles. waste manage. 2006; 8:99-108.

24. Widmer R, Oswald-Krapf H, Sinha-Khetriwal D, Schnellmann M, Boni M. Global perspectives on e-waste, Environ Impact Assess Rev. 2006; 25:436-458.

25. Betts K. Producing usable materials from e-waste, Environ Sci Technol. 2008; 42:6782-6783.

Chapter - 2
Cluster Establishment for Leveraged by using Combined Wireless Technologies

Authors

C. Silpa
Assistant Professor, Department of ECE, Malla Reddy Engineering College (A), Secunderabad, Telangana, India

Dr. A. Vani
Assistant Professor, Department of ECE, Chaitanya Bharathi Institute of Technology, Hyderabad, Telangana, India

K.S. Indrani
Assistant Professor, Department of ECE, Institute of Aeronautical Engineering College, Secunderabad, Telangana, India

Chapter - 2

Cluster Establishment for Leveraged by using Combined Wireless Technologies

C. Silpa, Dr. A. Vani and K.S. Indrani

Abstract

The technological advancement has led the whole world to be smarter and wiser with the use of intelligent machines. In the transportation industry, new innovations are creeping up day by day to ease the livelihood of man. Smart projects are in tremendous action throughout the world. Smart cities are coming up based on different projects implantation. One of them is employing a much safer world with ITS. In our research, a clustering algorithm is designed with the concept of utilizing LTE and DSRC, where a dynamic route discovery is employed in which the location of nodes, base stations, and the nodal powers are collected. The introduction of LTE Base station in our proposition actuated physical importance which tends to the capacity confinements of DSRC as far as distance connectivity is concerned. In view of the location and the battery control, the route discovery process is done occasionally. Keeping in mind the end goal to enhance the propagation delay, transmission capacity and cluster life time, cluster protocol is proposed. Simulation results demonstrate that our convention can outperform the existing standard as far as the end to end packet delivery ratio and latency.

Keywords: LTE, DSRC, VANET

1. Introduction

At the point when standards of MANET are employed in the domain of vehicles, they formed VANETs. A traditional definition of VANETs is inter vehicle communication. The vehicles are embedded with sensors and communicate with other vehicles or the framework outside termed as Road Side Units. The issues pertaining to the formation of clusters in the vehicular environment has been tremendous research in the past few years. The most challenging issue is cluster maintenance in case of node mobility. A vehicular network is a type of network with a very high degree of mobility.

If we can think about the moving pattern of vehicles, they follow a specific pattern and normally shaped groups particularly on a single lane road or in case of dense traffics. Several issues and challenges are discussed like the technical challenges in the management of network, collision and congestion control, security then, social and economic related challenges. As vehicles are highly mobile as mentioned earlier, the formation of stable clusters is also one issue to consider during the process of clustering. Some of the open challenges in VANET clustering are the high degree of node mobility which leads to cluster instability, issues in data dissemination and security issues, collision and congestion control, horizontal and vertical handoff mechanisms, environmental changes like microwave access, multilevel clustering, cluster head changes, and cluster reorganization. A cluster in VANET is one of the plans utilized for making a VANET topology less dynamic. In this research, a clustering algorithm is presented that employs the location of nodes and base stations for route discovery with the end goal of enhancing propagation delay, transmission capacity and battery lifetime.

2. Clustering in VANET

As the network of vehicles possessed a dynamic topology, a vehicular network is likely to face stale entries and overcrowding. So as to maintain a strategic distance from these sorts of issues numerous arrangements have been proposed of which clustering is one of the arrangement methods. Clustering decreases the count of messages and expands the system network. A few clustering algorithms are reviewed which are discussed in the following. Jaskaran Preet Singh *et al*. mentioned in the idea of the number of connections and vehicular mobility utilized for cluster arrangements and for electing cluster head. Amid the cluster arrangement, hubs with a generally higher level of availability, at first formed a structure that is assigned as leadership. The leadership at that point takes an interest in the election of cluster head and effective cluster re-association utilizing the total relative speed of vehicles. Mobility-based clustering algorithm (MOBIC) is a prevalent clustering algorithm referenced in different investigations. This methodology depends on the most minimal ID calculation; yet, it utilizes a flag control. Level mobility metric that is retrieved from successive receptions. Wolny displayed an advanced modified distributed mobility adaptive clustering algorithm (Modified DMAC) to adjust to the new highlights of VANET. It varies in the method for distinguishing topology changes. There is no requirement for any lower level administration that would be in charge of finding join manifestations and disappointments. Rather, the calculation depends on periodical sending of HELLO messages.

Ucar *et al*. presented a vehicular multi-hop algorithm for stable clustering (VMaSC) in light of picking the vehicle with the least mobility. Mobility is determined by taking the distinction in speed among neighboring vehicles in multi-hops. In any case, VMaSC requires the help of GPS or comparable area administrations to get mobility information. DMCNF enables vehicles to occasionally pick their targets from onehop neighbors in a disseminated way. The neighborhood follows procedure considers relative mobility, increasingly dependent on the number of followers, and additionally dependent on the historical/stored data. This procedure improves the dependability of clusters amid system advancement. The distributed manner of picking a target prompts simple support of the cluster organization.

3. Proposed weighted value clustering (WVC) algorithm

Clustering in VANET implies framing vehicles into little arrays dependent on some normal qualities or attributes, for example, vehicle's course, velocity and so on. Because of the progressive topology transition, the cluster's support is feeble and variations of cluster head is inevitable. The principle paradigm for cluster layout is to restrain the overhead and augment cluster's constancy. The increase in cluster head lifetime and the restriction imposed on cluster group reorganization can lead to a cluster strength. In any clustering algorithm, the most vital task is the arrangement of clusters with efficient bandwidth usage. VANET Architecture with Smart Car In this particular section, a novel design scenario is proposed for vehicular correspondence envisioned in Figure. 1. It is anticipated that all vehicles are fitted with GPS (Global Positioning System) for uncovering a vehicle.

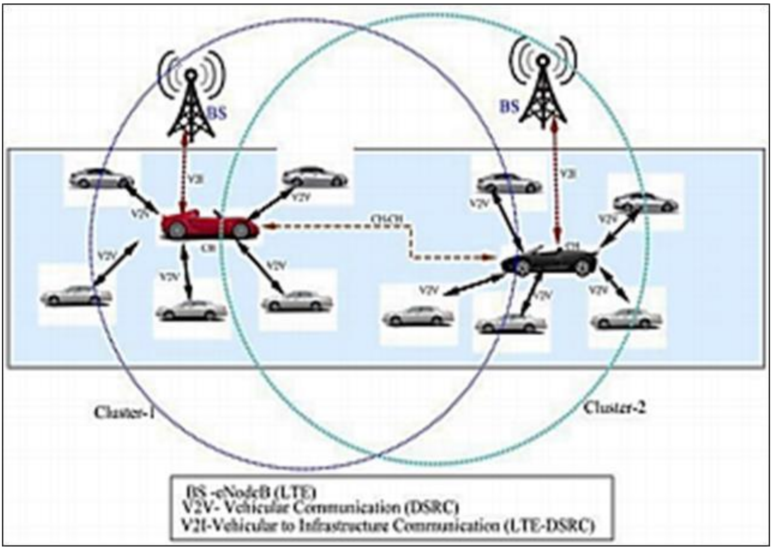

Fig 1: Vehicular Network Scenario

In our proposed architecture, LTE cellular infrastructure acts as RSUs for communicating with vehicles and OBUs are the vehicles with DRSC capabilities antennas. An RSU should remotely transfer and download information from and to vehicles utilizing IEEE 802.11p and LTE hybrid communication strategy as proposed. It is assured that RSU is placed at a distance of 4-5Kms and the vehicles within 1Km proximity can communicate among themselves using DSRC and those which do not fall in this proximity can communicate using LTE. The OBUs can analyze the retrieved data and then disseminate to the other vehicle OBUs within its vicinity. Among two RSUs, the data are disseminated from an OBU to another in a multihop fashion. The proposed architecture for the urban scenario is shown in Figure. 2, which is imported from a traffic simulator tool named Simulation of Urban Mobility (SUMO) of an intersection picturesque of Khyndailad commonly known as Police Bazaar located in Shillong in India.

Fig 2: Police bazaar map imported from Open Street Maps and SUMO

There are certain classifications during cluster formation and in this proposition, a few definitions are explored for cluster formation which are described below.

1) **Cluster Head (CH):** A CH will embrace as a hand-off for dissipating information to the individual clusters from the BS and from the Cluster Members (CMs) to the BS.
2) **Cluster Member (CM):** CMs are the vehicles inside a cluster which is under the area of a specific BS. CMs can connect with the BS through the CH, where the CH will exchange the information. Other than this, the CM can likewise connect with each other in 1-hop, when a similar message should be transferred in 2-hop the beacon packets should not be altered otherwise the second CM may get stale messages.

4. Cluster head selection

The introduction of LTE Base station in our proposal induced a physical significance which addresses the capacity limitations of DSRC in terms of distance connectivity. For Cluster Head selection two scenarios come into the picture.

a) Scenario 1

LTE Base Station as the Cluster Head In this particular scenario, with the presence of LTE Base station, LTE BS is considered to be the cluster head taking into account rural areas where sparse vehicles are presently provided the speed of the vehicle is much more as compared to those vehicles in the urban scenario. Based on the geographic location of placing the LTE tower, when the BS sense vehicles in its vicinity it will broadcast a message with its unique identifier along with a message that the particular vehicle is in its vicinity; then automatically that particular vehicle will be a cluster member. Hence, in this way cluster can be established.

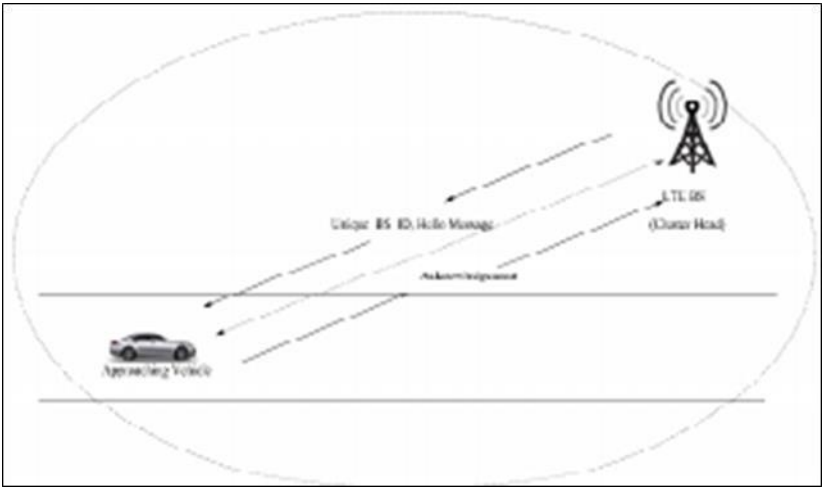

Fig 3: Scenario 1: LTE as CH (Rural Areas)

b) Scenario 2

Smart Vehicles as Cluster Head In this scenario, we considered the urban areas where vehicles move at uniform speed and in fact lower speed as compared to rural areas. Therefore, cluster establishment is quite easier and stable clusters can be formed. So as to reduce network traffic or substantial demands in the BS, vehicles inside the cluster will be nominated as a cluster head dependent on the algorithms clarified in the later sections. Figure 4. depicts the vehicles as CH and information is relayed in the cluster via the CH.

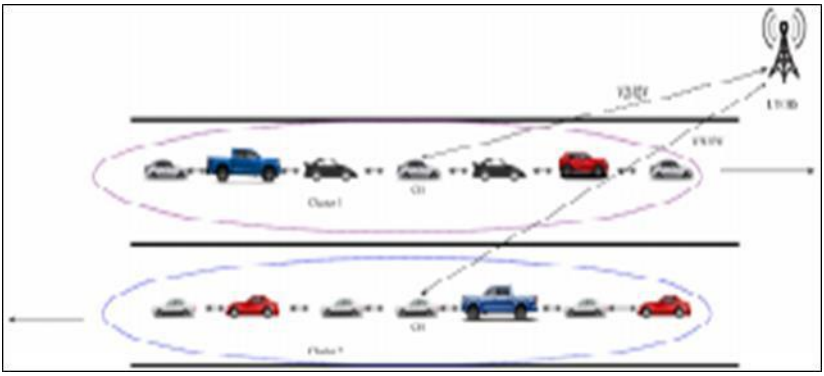

Fig 4: Scenario II: Vehicle as CH (Urban Areas)

In our proposed work, rather than a solitary CH, a cluster comprises of various leader nodes which are assigned as cluster heads. The CH is chosen

dependent on the radius with the base station. It is similar to the cluster head selection proposed.

The following procedure is executed for forming clusters and for selection of cluster head. Let V = V1, V2, V3…, Vn be an array of vehicles moving on the road equipped with DSRC transceivers.

Let C = C1, C2, C3, ……Cn be the cluster head classes. The primary action is to figure the distance of separation and orientation of a particular vehicle when it enters a particular locale. Before finding out the course, distance should be resolved first which can be processed.

5. Experimental results and discussion

By using The Simulator Urban Mobility (SUMO) version 0.25.0 traffic generator and NS2.35, we executed our proposed work in terms of the different performance metrics. 4.4.1 Simulation Setup Scenario We setup a scenario of simulation with 1000m x 1000m region in ns-2.35 version. The network animator (NAM) and tracing files are used for the VANET concept in NS2 simulation. The model depends on the current 802.11p and the other model is estimated in terms of hybrid communication where IEEE 802.11p and LTE are considered in which distance of separation is contemplated so as to approve the enhancement of communication. The existing model is represented as 802.11p during simulation and the other is represented as Hybrid with the parameter name. The parameters used in ns2.35 for VANET simulation are outlined in Table. 1 based on IEEE 802.11p standard.

Parameter	Specifications
Network Simulator	ns-2.35
Visualization Tools	Tracefile, NAM
Simulation Area	1000m x 1000m
Channel Type	Wireless Channel
Propagation Model	Two Ray Ground
Network Interface Type	Phy/NlirelessPhy
Antenna Model	Omni Antenna

In a typical wireless network, incessant activity is a definitive objective. Given the exceedingly portable aspect of a vehicular system, persistent availability has turned into a vital research challenge that is at present accepting huge consideration. In a request to build the network of a VANET, a conceivable arrangement is to convey numerous roadside units (RSUs) close to long roadway portions. It is imperative to take note of that in a vehicular system, an RSU can communicate with infrastructures, also,

whenever required, an RSU can dispense correspondence channels to vehicles inside its proximity. Besides, RSUs are vital operators for data dispersal in a vehicular system. In order to expand the inclusion scope of a VANETs' remote hubs (i.e., vehicles and RSUs), the certainties exhibit that broadening the inclusion scope of vehicle's radios may enlarge the accessibility region of a framework; nevertheless, this game plan is connected with a couple of weaknesses, for instance, lesser information rates and increased packet collision, which may result in elevated conveyance delays. In both proposed courses of action, the framework requires extensive energy, which isn't constantly available [79]. Honestly a dependable source of energy is given to vehicles by their electric motor; nevertheless, it is astonishingly expensive to give organize control relationship with RSUs in specific areas. This is a basic limit to the engagement of a vehicular framework. In certain vehicular organizing applications, for example, crash evasion, DSRC with LTE are joined to make use of both of their supremacy. Consequently, optimum cluster management can be utilized to diminish the power utilization of Inter-Vehicle Communication (IVC) by intermediary deciding strategies. Therefore for energy consumption of various nodes as we are already aware the Total energy consumed is the product of total power and time. Similarly, in our proposal, this basic formula is used for the calculation of the energy consumption of each node. A comparative analysis is shown in Figure 5.

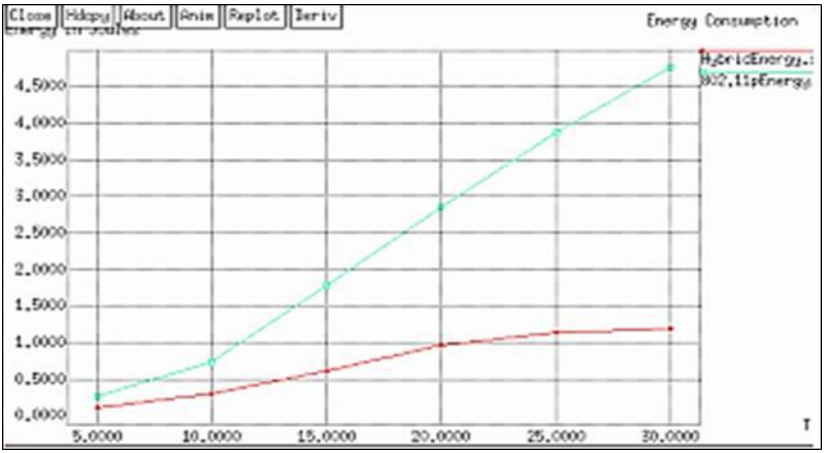

Fig 5: Mobile Nodes Power Consumption

An end-to-end delay (E2E delay) in system topology is the time taken by the packet to arrive at the objective destination. We compute end-to-end for any two vehicles in a rectangular lattice topology as follows:

E2Edelay = delay1 + delay2 +.... + delay n

In information conveyance was scrutinized from starting point to target in VANETs and it has been justified that for a solitary crossing point, the information conveyance delay can be diminished by selecting pertinent relay nodes. The end-to-end delay has been simulated using NS2, where a comparative conclusion between the existing scheme and the proposed scheme has been discussed in the following section.

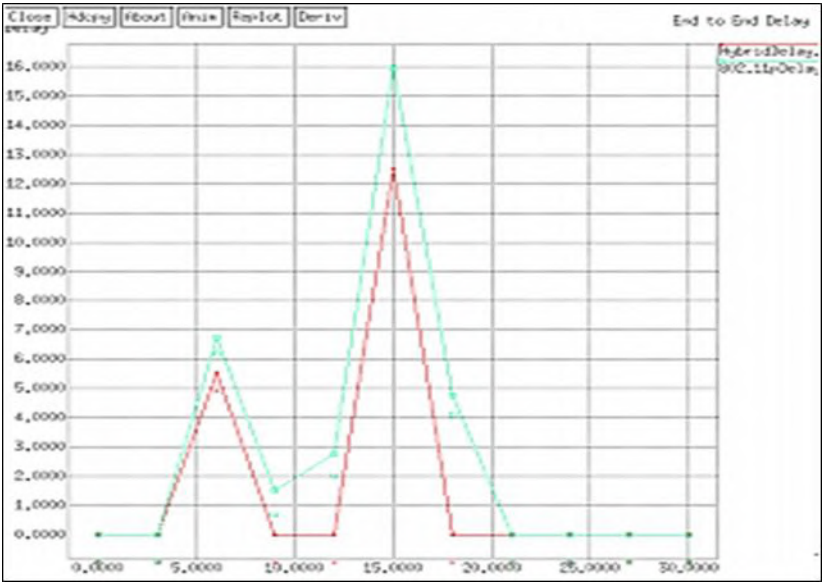

Fig 6: End-to-End Delay vs the number of nodes

Figure 6 delineated that, with an increase in traffic density, the end-to-end delay diminishes nearly to the existing scheme. This is on the grounds that an increase in traffic density increases the probability of packets being directed as opposed to being caught in suspension buffer. The fact that end-to-end delivery is comparatively lower in a hybrid infrastructure rather than the existing infrastructure as only the cluster heads communicate with the Base station, hence less traffic congestion is observed at the LTE BSs.

In the simulation scenario, we have taken a number of vehicle nodes to measure the throughput parameter in VANETs. In this paper, an average throughput is computed by taking the received packet and its size with respect to time. The number of nodes with their corresponding generated through put for VANET is summarized in Table.2 utilizing X graph.

Table 2: Number of Nodes with generated Throughput

Number of Nodes	Throughput
5	0.5556
10	1.1112
15	1.43
20	4.686
25	4.686
30	4.686
35	4.686
40	4.686
50	4.686

Mohammad Nekoui *et al.*, mentioned in that the road geometry enormously influences the throughput of VANET. Consequently, we presented a distance constrained throughput in a solitary road framework and within the availability of infrastructure dependent on unicast correspondence in VANET. In throughput performance effectiveness is demonstrated by analysing the distribution of contents from the source vehicle to multiple relay vehicles with the largest mobility diversity inorder to improve concurrent transmissions.

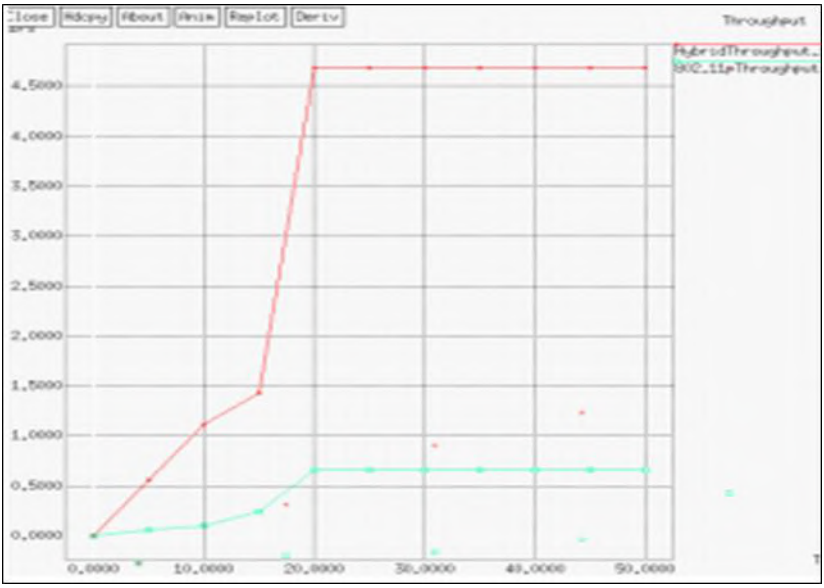

Fig 7: Throughput vs Number of nodes

Conclusion

From the above result analysis, it is found that the performance of VANET based on weighted value with throughput parameter is better than using 802.11p standalone standard.

References

1. Nabih Jaber, Nicholas C Doyle, Kemal E Tepe. New Combined WiMAX/DSRC infrastructure design for efficient vehicular networking, EURASIP Journal on Wireless Communications and Networking. 2012; 1(1):1-26.
2. History of ITS: Connected Vehicles and Smart Cities, Egan Smith, Managing Director, ITS Joint Program Office, U.S. Department of Transportation, 2017.
3. Biswas FS, Tatchikou R. Vehicle-to-vehicle wireless communication protocols for enhancing highway traffic safety, IEEE Communication Magazine. 2006; 44:74-82.
4. Guerrero-Ibanez, Juan Antonio, Sherali Zeadally, Juan Contreras Castillo. Integration challenges of intelligent transportation systems with connected vehicle, cloud computing and internet of things technologies, IEEE Wireless Communications. 2015; 22(6):122-128.
5. Zhan Y, Moustafa H. Vehicular Networks Techniques, Standards and Applications, Taylor & Francis Group, LCC, 2009. ISBN: 978-1-4200857-1-6.
6. "Indian Traffic Rules and Fine Lines", 2018.
7. url: https://www.worldbank.org/en/topic/transport/brief/connectionsnote-26
8. nptel.ac.in/courses/CSE/IIT Kharagpur.
9. url: https://www.theconversation.com/intelligent-infrastructurewhen-roads-and-vehicles-tralk-to-each-other
10. Smart Transportation Alliance: url: https://smart-transportation.org.

Chapter - 3
Unit Commitment Problem with DGL and VPL

Authors

V. Lakshmi Devi
Professor, Department of EEE, S.V College of Engineering (Autonomous), Tirupati, Andhra Pradesh, India

Y. Hari Krishna
Assistant Professor, Department of EEE, S.V College of Engineering (Autonomous), Tirupati, Andhra Pradesh, India

K. Raju
Assistant Professor, Department of EEE, S.V College of Engineering (Autonomous), Tirupati, Andhra Pradesh, India

Raja Reddy Duvvuru
Associate Professor, Department of EEE, Malla Reddy Engineering College (Autonomous), Hyderabad, Telangana, India

Chapter - 3

Unit Commitment Problem with DGL and VPL

V. Lakshmi Devi, Y. Hari Krishna, K. Raju and Raja Reddy Duvvuru

Abstract

This work presents the Unit Commitment (UC) of generation and load dispatch with valve point loading effect. The main objective function is to minimize the operating cost with valve point effect a new approach to evaluate Unit Commitment Problem (UCP) including valve point loading effect is proposed, and it is used to determine the total generation cost for 24 hours schedule with constraints. The effectiveness of the proposed UCP with VPL has been tested in IEEE-30 bus system.

Keywords: UC, VPL, optimization

I. Introduction

In power system operation, UC problem is a main optimization problem. The objective of UC problem is to program the committed generating units to meet out the system load demand with minimum operating cost by satisfying the constraints. Thus, UC problem with valve point loading is represented as a non-linear optimization problem with satisfying the constraints. A particular load demand has existing at some instant of time in a power system, which could be supplied in an infinite number of configurations. Operating economy is naturally predominant in determining the best choice, besides several others evenly important factors should be considered. UC of power systems describes the selection of the finest operating configuration that provides the maximum operating economy or minimum operating cost. The total operating cost comprises fuel, labor and maintenance costs, but for simplicity, consider only fuel cost is considered for power production, as it formulates the major portion of the total operating cost and it is directly correlated to the value of power output. Different units of fuel cost characteristics could be different in giving different economic effectiveness. Thus, the problem of finest power flow of a power system can be stated as: shifting the load among the various units of generating stations and the overall operating cost of generation is reduced for a 24-hour demand.

In literature, for simplicity, each unit of the Unit Commitment Problem (UCP) has been approximately denoted by a single quadratic function and is resolved with mathematical programming techniques. These mathematical methods usually require the derivative information of the cost function. Due to valve point loading effect, the input and output characteristics of generating units are non-convex. Thus, the practical UCP should be represented as a non-convex optimization problem with constraints. It makes the challenge of determining the global optimum, and it cannot be directly solved by mathematical methods. This trouble has been solved by conventional methods. But, the drawback of those techniques is failed to get a global optimal solution.

Many hierarchical methods have been developed to solve these problems, considering the valve-point loadings. But, those methods have premature convergence characteristic. To obtain an accurate and practical solution for UCP, the realistic operation of the UC problem should be taken into valve-point effects. Walters & Sheble (1993) have first developed GA to ED trouble with VPL. Orero & Irving (1996) used GA with ED problem by prohibited operating zones to attain near global optimal solution. Sinha *et al*. (2003) proposed an EP technique for economic load dispatch. Victoire & Jeyakumar (2004) presented a HPSO sequential quadratic programming method for solving ED with VPL effect. Chiang (2005) implemented an improved GA for power economic dispatch of entities with VPL effect as well as multiple fuels. Coelho & Mariani (2006) have evaluated a combination of chaotic DE and quadratic programming for ED optimization with VPL effect method. Quantum inspired PSO for VPL economic load dispatch was developed by Meng *et al*. (2010).

This work presents a method for solving the UC problems with valve-point effects with DGL by using PSO. The results of the VPL with DGL are solved with and without load shifting. The outcomes show that the proposed PSO algorithm solves UC problems with the valve point effect. The outcomes exhibit that the algorithm could manage optimization problems.

II. UCP with VPL

The UC problem with valve point loading effects causes alteration in the objective function formulation. To determine the optimal fuel cost, a feasible and effective optimization technique may be utilized. The proposed approach is based on PSO algorithm which combines the benefits to give an optimal solution. In order to validate the proposed methodology, detailed simulation results obtained in IEEE-30 bus test systems are presented. The objective of UCP is to find out the optimal design settings of generators including the shut

down and start-up of cost to minimize the total operating cost without violating other operating constraints as stated by Sasaki *et al*. (1992). More than a small term period, UC in a power system required for calculating a shut down and start-up schedule of units to converge the predicted demand, suggested by Wood (1996). UCP determines which power generating units should be Committed/Decommitted over a planning horizon and it is generally continuing from a day to weeks and divides into periods of one hour. In an electric power system, due to the nature of human activities, customer loads are varied periodically. To manage with these repeated variations, the dispatcher has to switch on sufficient number of generating units to reach the load demands throughout each interval of scheduling horizon.

III. Problem formulation

UC problem assumes that there are N units already connected to the system. The purpose of UC problem is to find the optimum operating policy for these N units. The objective function of UCP is to minimize the generating cost. The fuel cost equation is given, in the conventional UCP, cost function is approximated by quadratic function. However, large system generators are affected by temperature effects, due to continuous operation of connected systems. This will cause non-linearity, discontinuity and non-convex problem. Hence, fuel cost curve is not within the boundary. To overcome this problem, quadratic equation is added with sine component for this proposed approach. The expression for the total fuel cost without DGL and with VPL is expressed as

$$\text{Min } f = \sum_{j=1}^{n} (a_i + b_i P_i + c_i P^2) + d_i * \sin\{e_i * P^{min} - P_i\}) \quad \ldots (1)$$

UC Problem with valve point loading effect with DGL

The main objective function of system operator is minimization of the total cost, while taking into the description with DGL along with valve-point loading effect with fulfilling constraints, and the expression is shown as

$$F = (FC_T + d_i * \sin\{e_j * P^{min}_j - P_j\}) + SU_T + LSC_T \quad \ldots (2)$$

Constraints

In case of UCP, the generations are considered as varying parameter. However, they are allowed to take values within specified limit to meet out a particular load demand. The total generation cost function is the function of individual generation of the units, which fulfill the constraints in 24 hours schedule. In this proposed method, the following constraints are considered.

A. Power balance constraint

In equality constraints, the total power generation must satisfy the load demand including transmission network loss. The proposed approach concentrates only load demand, P_L is not considered and it can be expressed.

B. Generator capacity constraints

In this constraint, the power generation of each unit should be within certain limit. It is not a necessary condition that the units are always available to share a load. In some cases, the units may be taken off, due, to maintenance. During the off-peak hours, it is not essential that the inefficient units are to be turn off. Considering these circumstances, there is a certain amount depending on shutting down and startup of a unit. The shutdown cost depends on shutting down a unit in the off-peak hours and startup cost depends on servicing it back on-line, during the peak hours. The expression can be given as

$$P_{G_j}^{min} \leq P_{G_j} \leq P^{max}, j = 1, ..., N_G \quad \ldots (3)$$

C. Start-up cost

The start-up cost takes place, when a generator unit is turned on. It depends on how long the generator unit has been shut down. If the generator unit has been turned off for a long period, a cold start-up cost is used. But, the generator unit has been turned off for a short period and hot start-up cost is used. The expression for start-up cost is shown as

$$\text{Start-up cost} = \frac{\text{hot start cost if down} - \text{time} \leq \text{cold start hours}}{\text{cold start cost otherwise}} \quad \ldots (4)$$

D. Shut down cost

Generally for every unit, shut down cost is a constant value. In the standard system, shut down cost is taken as zero.

E. Minimum up/down time constraints (MUT/MDT)

Minimum up/down time confines specifies that a unit should be on/off for a particular number of hours before it can be turned off or fetched online.

IV. DGL Structure

The structure of the generation and load is presented in this section. In Dispatch of Generation and Load (DGL), loads from a large trade customer are viewed as a dispatchable resources related to generating units. Here, both generation and load can be optimized simultaneously, to plan the profile of the system load. In DGL formulation, the generating units and customers are

modeled symmetrically. From the customer's point of view, it is not easy to adjust the power consumption interval-by-interval, owing to the load characteristics of inter temporal characteristics. In this DGL model, the physical necessities of entity customers could be thoroughly recognized by accurately modeling the load profiles. So, the demand-side resources turn into more predictable for system operators and moreover, the demand-side resources and the generation can be coordinated more efficiently and accurately.

To express the readiness of the customers to alter their consumption modes, the concept of Load Shifting Cost (LSC) is initiated. The new settlement mechanism is planned, in which LSC of interested customer is paid to non-responsive customers. The benefit of this method is that the customers are directed to bid according to their LSC. Under such situation of scarce generation capability, the customers shift their loads from peak hours to off-peak hours and a rivalry market for load shifting price can be made based upon the proposed method.

V. Results and Discussions

The IEEE-30 bus test system including valve loading effect is used to solve the proposed algorithm. The parameters of the proposed PSO to solve the UC problem in the test cases are: Population size = 60, c_1 and c_2 2.5, 0.2 respectively, number of iteration = 1000. The proposed algorithm has been executed in MATLAB- 7 computing environment in an Intel i3-3217U CPU @ 1.80 GHz processor, 4GB RAM.

Test case: IEEE-30 bus system

The branch data and the bus data are taken from Alsac O (1973). The demand data for IEEE-30 bus test system are taken from Zhong H (2015), and it is given in Appendix 2. The slack bus of the system is chosen as bus 5 and bus 1 and bus 2 are signified by quadratic function models of generator fuel cost curves. The generator fuel cost curve coefficients of those two generators are taken from Ongsakul W (2007). The performance of this algorithm is tested for a one-day scheduling. Scheduling results of conventional UC with VPL before load shifting are given Table 5.1. Table 5.2 gives the generation schedule for 24-hour load demand including valve point effect into UC problem and Table 5.3 shows the fuel cost for 24-hour load demand. It is clear that there is a substantial increase in total cost while considering valve point loading effect. So, the valve point loading effect may be taken into contemplation for optimal calculations.

Table 1: UC result of IEEE-30 bus system for before load shifting with VPL

Unit No	1	2	3	4	5	6	7	8	9	10	11	12	13	14	15	16	17	18	19	20	21	22	23	24
1.	1	1	1	1	1	1	1	1	1	1	1	1	1	1	1	**1**	1	1	1	1	1	1	1	1
2.	1	1	1	1	1	1	1	1	1	1	1	1	1	1	1	**1**	1	1	1	1	1	1	1	1
3.	1	1	0	0	0	0	0	0	0	1	1	0	1	1	1	**1**	1	1	1	0	0	1	1	1
4.	0	0	0	0	0	0	0	0	0	0	0	0	0	0	0	**1**	0	0	0	0	0	0	0	0
5.	1	0	1	1	1	1	1	1	1	1	1	1	1	1	1	**1**	1	1	1	1	1	1	1	1
6.	1	0	1	1	1	1	1	1	1	1	1	1	1	1	1	**1**	1	1	1	1	1	1	1	1

Table 2: Generation schedule of IEEE-30 bus system for 24 hour before load shifting with VPL

Unit No	Power Generation (MW)																							
	1	**2**	**3**	**4**	**5**	**6**	**7**	**8**	**9**	**10**	**11**	**12**	**13**	**14**	**15**	**16**	**17**	**18**	**19**	**20**	**21**	**22**	**23**	**24**
1.	80	42.3	75	80	78	80	60	70	80	80	80	80	80	50	80	80	80	79.9	80	80	80	80	80	80
2.	30	62.1	30	35	30	30	30	30	30	30	30	80	62	80	80	80	80	60.1	80	50	55	30	62.1	30
3.	15	10.6	0	0	0	0	0	0	0	10	20	0	28	50	50	50	50	50	10	0	0	30	17.9	30
4.	0	0	0	0	0	0	0	0	0	0	0	0	0	0	0	10	0	0	0	0	0	0	0	0
5.	30	30	30	30	30	30	30	30	30	30	30	30	30	30	30	30	30	30	30	30	30	30	30	30
6.	30	30	30	30	30	30	30	30	30	30	30	30	30	30	30	30	30	30	30	30	30	30	30	30

Table 3: Fuel cost of IEEE-30 bus system for 24 hour before load shifting with VPL

Hour	**1**	**2**	**3**	**4**	**5**	**6**	**7**	**8**	**9**	**10**	**11**	**12**
FC_T ($)	38526	35693	32336	35413	33240	33843	27806	30829	33843	36964	40088	49418
Hour	**13**	**14**	**15**	**16**	**17**	**18**	**19**	**20**	**21**	**22**	**23**	**24**
FC_T ($)	52525	55970	65045	68351	65045	58794	52539	40088	41630	43213	49400	43213
Total cost = $1063812												

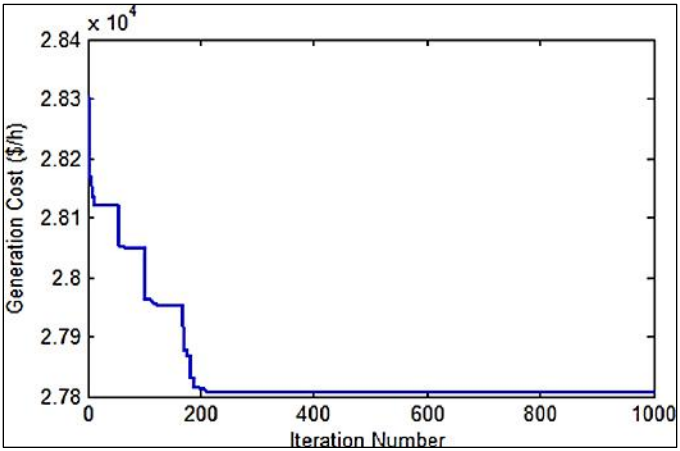

Fig 1: Seventh hour convergence characteristics of before load shifting

Scheduling results of conventional UC of DGL with VPL after load shifting are shown in Table 4. The generation schedule and corresponding fuel cost of IEEE-30 bus system after load shifting for 24-hour load demand are shown in Table 5 and Table 6, respectively. In before load shifting, the demand of sixteenth hour is huge and so, the fuel cost of the hour is high that causes the increase in overall operating cost. Hence, to decrease the operating cost for twenty-four-hour schedule, a part of the load (10MW) from sixteenth hour, in unit 4 is shifted to seventh hour in the first unit and thereby the overall operating cost becomes reduced by after load shifting. The operating cost for 24-hour schedule with before load shifting is $1063812 and the operating cost for 24-hour schedule with after load shifting is $1060509.

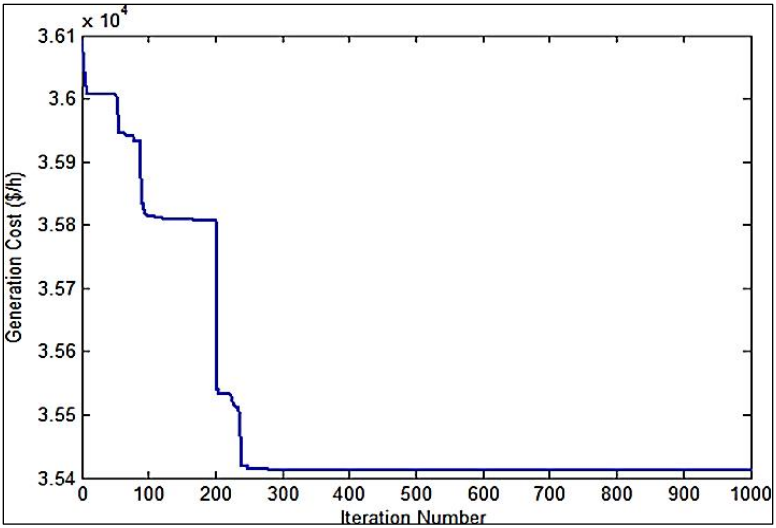

Fig 2: Seventh hour convergence characteristics of after load shifting

Figure 1 and Figure 2 represents, the convergence characteristics of seventh hour schedule for before load shifting and after load shifting, respectively.

Table 4: UC result of IEEE-30 bus system for after load shifting with VPL

Unit No	**1**	**2**	**3**	**4**	**5**	**6**	**7**	**8**	**9**	**10**	**11**	**12**	**13**	**14**	**15**	**16**	**17**	**18**	**19**	**20**	**21**	**22**	**23**	**24**
1.	1	1	1	1	1	1	1	1	1	1	1	1	1	1	1	**1**	1	1	1	1	1	1	1	1
2.	1	1	1	1	1	1	1	1	1	1	1	1	1	1	1	**1**	1	1	1	1	1	1	1	1
3.	1	1	0	0	0	0	0	0	0	1	1	0	1	1	1	**1**	1	1	1	0	0	1	1	1
4.	0	0	0	0	0	0	0	0	0	0	0	0	0	0	0	**0**	0	0	0	0	0	0	0	0
5.	1	0	1	1	1	1	1	1	1	1	1	1	1	1	1	**1**	1	1	1	1	1	1	1	1
6.	1	0	1	1	1	1	1	1	1	1	1	1	1	1	1	**1**	1	1	1	1	1	1	1	1

Table 5: Generation schedule of IEEE-30 bus system for 24 hour after load shifting with VPL

Unit No	Power Generation (MW)																							
	1	**2**	**3**	**4**	**5**	**6**	**7**	**8**	**9**	**10**	**11**	**12**	**13**	**14**	**15**	**16**	**17**	**18**	**19**	**20**	**21**	**22**	**23**	**24**
1.	80	42.3	75	80	78	80	70	70	80	80	80	80	80	50	80	80	80	79.9	80	80	80	80	80	80
2.	30	62.1	30	35	30	30	30	30	30	30	30	80	62.1	80	80	80	80	60.1	80	50	55	30	62.1	30
3.	15	10.6	0	0	0	0	0	0	0	10	20	0	27.9	50	50	40	50	50	10	0	0	30	17.9	30
4.	0	0	0	0	0	0	0	0	0	0	0	0	0	0	0	0	0	0	0	0	0	0	0	0
5.	30	30	30	30	30	30	30	30	30	30	30	30	30	30	30	40	30	30	30	30	30	30	30	30
6.	30	30	30	30	30	30	30	30	30	30	30	30	30	30	30	30	30	30	30	30	30	30	30	30

Table 6: Fuel cost of IEEE-30 bus system for 24 hour after load shifting with VPL

Hour	**1**	**2**	**3**	**4**	**5**	**6**	**7**	**8**	**9**	**10**	**11**	**12**
FC_T ($)	38526	35693	32336	35413	33240	33843	30829	30829	33843	36964	40088	49418
Hour	13	14	15	16	17	18	19	20	21	22	23	24
FC_T ($)	52525	55970	65045	65045	62031	58788	52539	40088	41630	43213	49400	43213
Total cost = $1060509												

Table 7: Generation schedule for before load shifting (only load shifting hours)

Hr	**Power Generation of units (MW)**						**LSC_T**	**FC_T**
	P1	**P2**	**P3**	**P4**	**P5**	**P6**	**($)**	**($)**
7	60	30	0	0	30	30	0	27806
16	80	80	50	10	30	30	-	68351
17	80	80	50	0	30	30	-	65045
18	80	80	30	0	30	30	-	58788
Total cost = $219990.00								

The total operating cost of 7th, 16th, 17th and 18th hour schedule before and after load shifting for IEEE-30 bus is given in Table 7 and Table 8, respectively. The before load shifting of fuel cost for the above said hour is $219990, LSC is zero and correspondingly after load shifting of fuel cost for the hours 7th, 16th, 17th, and 18th is $216693, and the load shifting cost is $450. Hence, the difference between before and after loading shifting cost for 7th, 16th, 17th and 18th hour is $3297. Table 9 shows the comparison of before and after load shifting for 24-hour scheduling. It is clear that the total operating cost of before load shifting is $241190 and after load shifting is $233343. So, the difference between before and after load shifting is $7847. This indicates that the cost of generation can be reduced by shifting the load. Therefore, it is economically feasible. Figure 3 and Figure 4 illustrate the convergence characteristics of sixteenth hour schedule for before load shifting and after

load shifting, respectively. It can also be observed that it converges to a fine value.

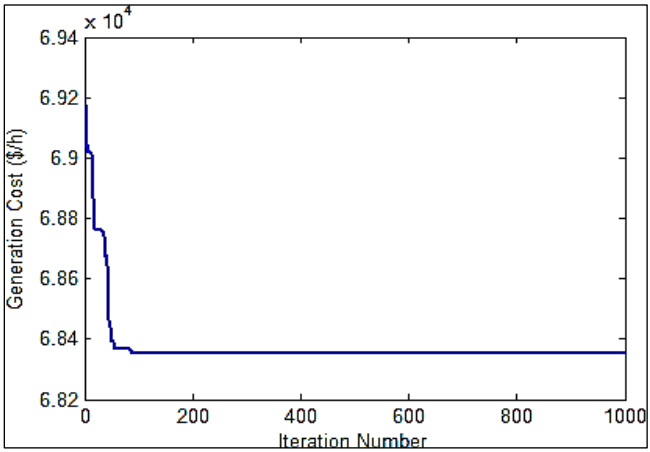

Fig 5.3: Sixteenth hour convergence characteristics of before load shifting

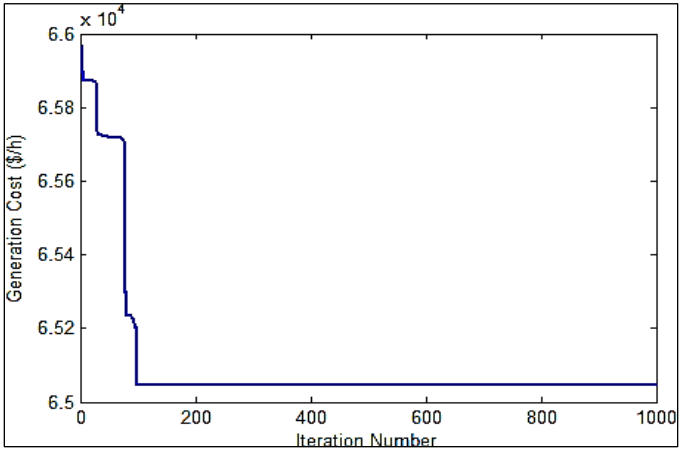

Fig 4: Sixteenth hour convergence characteristics of after load shifting

Table 8: Generation schedule for after load shifting with VPL

Hr	Power Generation of units (MW)						LSC_T	FC_T
	P1	**P2**	**P3**	**P4**	**P5**	**P6**	**($)**	**($)**
7	**70**	30	0	0	30	30	450	30829
16	80	80	50	0	30	30	-	65045
17	80	80	50	0	30	30	-	62031
18	80	80	30	0	30	30	-	58788
Total cost = $216693								

Table 5: Comparison of before and after load shifting with VPL

Cost ($)	Before Load Shifting	After Load Shifting
Operating cost	219990	216693
Start-up cost	21200	16200
Load shifting cost	0	450
Total Cost	241190	233343
Benefit	-	7847

Figure 5 shows the total operating cost comparison of before and after load shifting. Though the LSC is added, the start-up and operating costs on the generation part are reduced. Finally, the overall cost is reduced and it turns to economically beneficial.

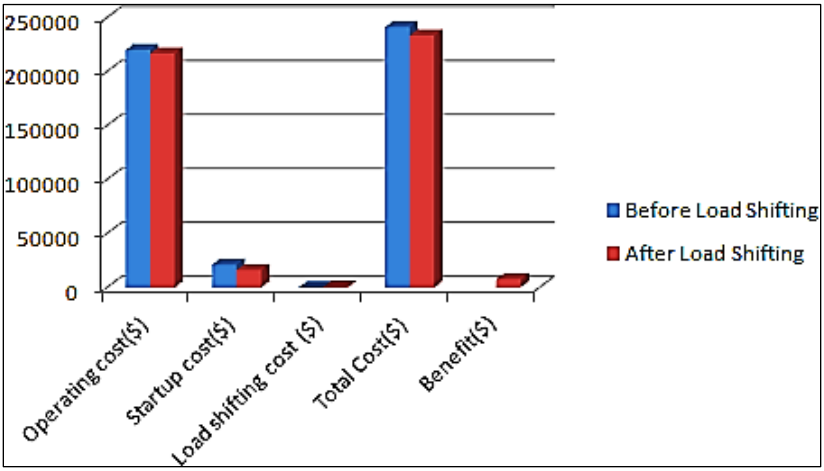

Fig 5: Graph for before and after load shifting

Conclusion

In this work, a PSO algorithm with DGL and valve point loading effect has been proposed. To show the effectiveness of the algorithm, it is applied in unit commitment problem with six generating units. This method has many advantages because the generation limit, power balance and constraints like minimum down / up time are incorporated in the problem formulation. In DGL, LSC is initiated to state the excitement of the customers to alter their load models. The DGL is formulated in which, the reply behaviors of consumers, like load shifting can be clearly modeled. Moreover, a new settlement mechanism is also presented, in which the load shifting costs of responsive consumers are remunerated by non-responsive consumers. The proposed method helps the consumers to bid related to their actual LSC. The

proposed method is tested in standard IEEE-30 bus system. The total cost obtained from the proposed method for before load shifting is $241190, and after load shifting is $233343. The cost benefit is $7847 where as the cost benefit of UC problem with DGL without considering VPL is $4819. Thus, the results show that the proposed algorithm is capable of optimizing the total fuel cost with valve point loading effect.

References

1. Aalami HA, Parsa M, Moghaddam. Demand response modelling considering interruptible/Curtailable loads and capacity market programs, Applied Energy. 2010; 8(7):243-250.
2. Abido MA. Optimal power flow using particle swarm optimization, in Elsevier Electrical Power & Energy System. 2002; 24:563-571.
3. Abido MA. Multi objective optimal VAR dispatch using strength Pareto evolutionary algorithm, In IEEE Congress on Evolutionary Computation Sheraton Vancouver Wall Centre Hotel, Vancouver, BC, Canada, 2006.
4. Abookazemi K, Ahmad H, Tavakolpour A, Hassan MY. Unit commitment solution using an optimized genetic system, International Journal of Electrical Power & Energy Systems. 2011; 33(4):969-975.
5. Abou El, Ela A, Abido MA, Spea S. Optimal power flow using differential evolution algorithm, In Elsevier Electrical Power System Research. 2010; 80:878-885.
6. Adapa R, El-Hawary ME, Momoh JA. A review of selected optimal power flow literature to 1993, Part I: Nonlinear and quadratic programming approaches, in IEEE Trans. Power System. 1999; 14(1):96-104.
7. Aguado JA, Quintana VH, Conejo AJ. Optimal power flows of interconnected power systems, in Proc. IEEE Power Engineering Summer Meeting. 1999; 2:814-819.
8. Albadi MH, El-Saadany EF. A summary of demand response in electricity market, Electric Power Systems Research. 2008; 7(8):1989-1996.
9. Al-Rashidi MR, El-Hawary ME. Applications of computational intelligence techniques for solving revived optimal power flow problem, Electr. Power Syst. Res. 2009; 79(4):649-702.

Chapter - 4
Effect of Doping on Optical Properties of ZnO Thin Films

Authors

Rani Maddula
Assistant Professor, Department of Physics, Sri Indu College of Engineering and Technology, Hyderabad, Telangana, India

Kesava Vamsi Krishna
Associate Professor, Department of Physics, Malla Reddy Engineering College (A), Hyderabad, Telangana, India

Chapter - 4

Effect of Doping on Optical Properties of ZnO Thin Films

Rani Maddula and Kesava Vamsi Krishna

Abstract

In this work, studies on optical properties of doped ZnO thin films with Al, Sn, Sb and Cu are presented in detail. The variation in transmittance due to doping are discussed and optical absorbance of the films are analyzed to elucidate the bandgap through Tauc plots. Further, this chapter provides information on transient photoconductivity of the doped films under visible and UV region of wavelength. The influence of dopant in photoluminescence spectra of ZnO thin films is outlined.

I. Introduction

Studies on optical behaviour of semiconductor thin films mainly involve optical absorption, transmission and reflection properties. The optical absorption spectrum facilitates a simple way to interpret the optical band gap of the material which may be direct or indirect depending on the electronic transition between the energy levels. The semiconductors possess distinctive band structure with Fermi energy lying between conduction and valence band in the band gap. For a pure undoped semiconductor, Fermi energy lies halfway between valence band maximum (VBM) and conduction band minimum (CBM). Materials in which valence band maximum (VBM) and conduction band minimum (CBM) lie on the same value of k-vector, possess direct band gaps whereas materials in which VBM and CBM do not occur for the same value of k have indirect band gaps, which involve the electronic transitions supported by phonons [1-3].

As a wide direct bandgap II-VI binary semiconductor compound (E.g. ~ 3.3eV), ZnO is a favourable candidate for blue/UV optoelectronic, lasers and detectors. The shorter wavelength associated with it enables higher storage density in optical storage systems as storage density is inversely proportional to square of the wavelength. Further, as blue or UV light emitters, ZnO could be used in white solid-state lighting by using them to excitephosphors. Moreover, ZnO is found transparent to visible light and can

be employed as transparent transistors for optical circuitry for colour displays [4-7].

It has been observed that photoresponse of n-type metal oxide semiconductors like ZnO show slow conduction decay process. ZnO films in general exhibit Photoluminescence 'near band edge emission' (NBE) and a deep level blue-green emission. Direct bandgap materials exhibit better luminescence efficiency related to recombination of electrons and holes leading to emission of photons. These properties can be used to make devices in UV or blue emission. Even though controversy exists regarding blue-green emission, many researchers have reported that UV emission is the outcome of excitonic emission [7-9].

In this chapter, a comparative study of the optical properties of ZnO thin films on doping with Al, Sn, Sb and Cu has been carried out and is detailed. The variation in photoresponse with different dopants under visible and UV light is elaborated and as part of defect study, Photoluminescence spectra are analyzed for typical samples of each dopant.

II. Experimental techniques

The absorption spectra of the films are recorded in the wavelength range 300-1200 nm using a UV-Vis-NIR spectrophotometer of model JASCO V-570 having a double beam system with single mono chromator, containing deuterium and halogen lamps. The film thickness is measured by Fizeau's interferometric technique and is also verified using Stylus profilometer. The thickness of different films used for the present study varies from 100 to 160 nm. For the photo response measurements an FHS quartz halogen lamp is used along with a Keithley 2611A source meter. Photoluminescence spectra are recorded using Model: Fluoromax-4C spectro fluoro meter with the excitation wavelength of 325nm.

A. Results and Discussion

i) Optical properties of ZnO: Al thin films

In the present investigation, as mentioned in previous chapters, Zinc is doped with Aluminium at different concentrations and samples showing distinct variations in optical properties are chosen for further detailed optical studies. The lightly doped (~1 at%) ZnO sample is designated as ZnO:Al-1, moderately doped (~3 at%) as ZnO:Al-2 and heavily doped (~10 at%) as ZnO:Al-3 throughout this work.

Optical absorption and transmission

Al-doped ZnO thin films are widely used for its extensive transmittance as transparent conductive electrode. In the present study, the optical properties of the films are investigated for UV-Vis range. The absorbance graph of the undoped and Al doped ZnO samples are represented in Figure. 1(a). The fundamental absorption edges in the spectra of undoped and Al doped samples characterize the excitation of electron from valence band to conduction band. Figure. 1(b) illustrates transmission spectrum of both undoped and doped ZnO thin films which indicates an improved transparency for lightly and moderately doped samples ZnO:Al-1 and ZnO:Al-2 respectively and heavy doping at 10 at% Al shows moderate transparency. The optical band gap is determined from Tauc's formula given by equation and Figure.2 displays the optical bandgap of both undoped and Al doped samples. Sharma and Khare [10] have reported blueshift in bandgap on doping ZnO with Al. In the present study, doping up to 3 at% Al in the ZnO samples exhibit a blueshift in bandgap while heavy doping at 10 at% Al reduces bandgap sharply. Seeber *et al*., [6] have reported that doping of ZnO thin films with Al impurities increases conductivity of ZnO films and because of Burstein-Moss effect the absorption edge shifts to higher energy side which results in widening of optical bandgap. The decrease in bandgap of the sample with 10 at% Al may be due to heavy defect formation which produces intermediate defect levels. Redshift in E.g. has been reported by Caglar *et al*., and Oh *et al*., at heavy doping of Al [7, 10-12]. The values of bandgap of undoped and doped ZnO samples are listed in Table. 1.

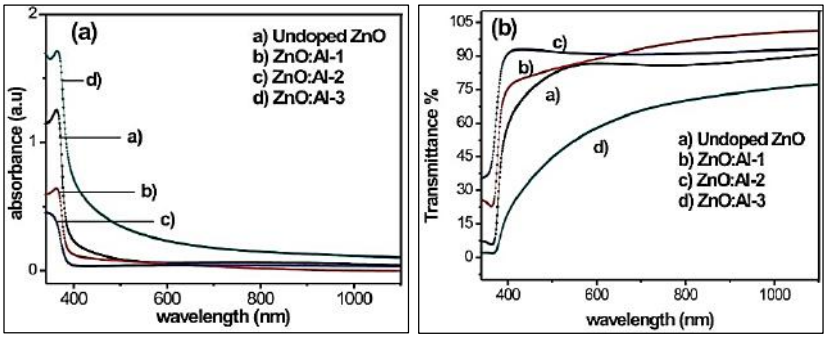

Fig 1: a) absorbance spectra b) transmittance spectra of undoped and Al doped ZnO samples

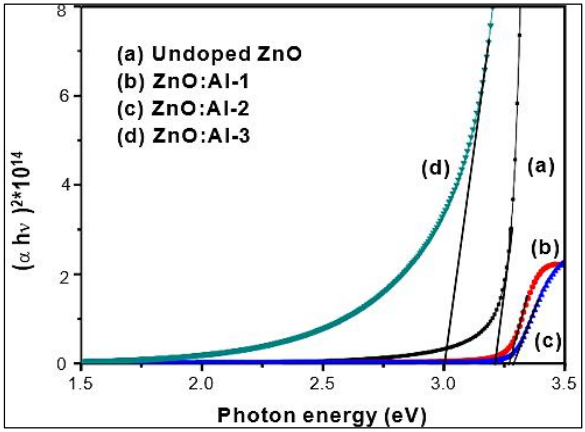

Fig 2: Tauc's plot showing optical bandgap of undoped and Al doped ZnO thin films

1. Photosensitivity studies

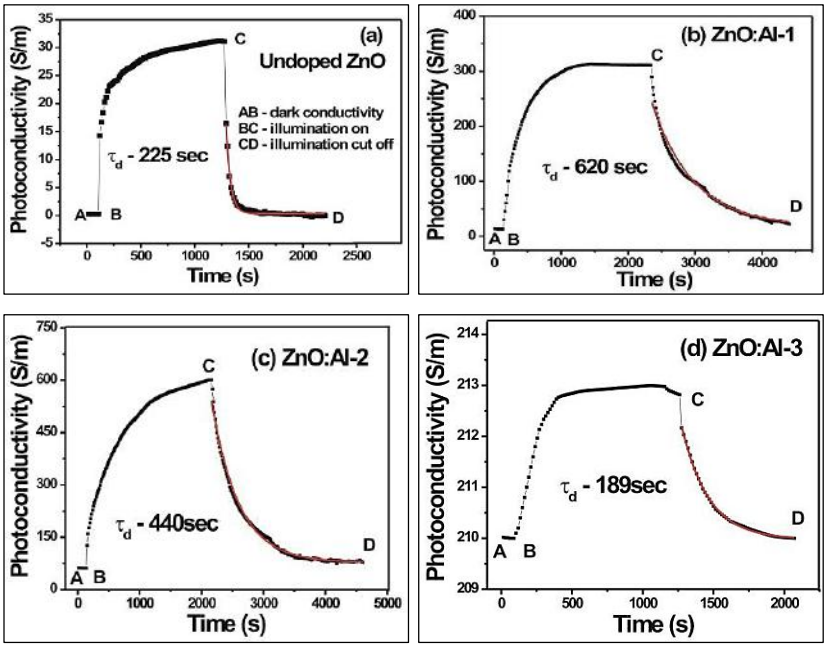

Fig 3: a-d) Photoresponse of undoped and Al doped ZnO thin films under visiblelight

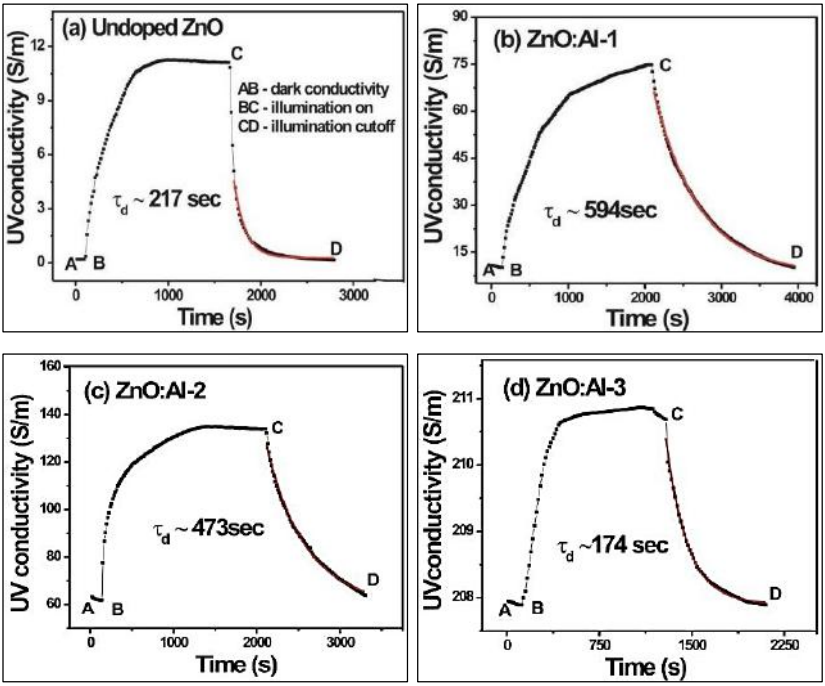

Fig 4: a-d) Photoresponse profile of undoped and Al doped ZnO thin films underUV light

Figure. 3(a)-(d) shows photoconductivity Vs time curve of both undoped and Al doped ZnO thin films under visible light. For ZnO thin films, even though the samples show systematic increase in room temperature conductivity, a similar variation is observed only for samples ZnO:Al-1 and ZnO:Al-2 with ~1 at% and ~3 at% while the heavily doped samples with ~10 at% Al show little photoresponse. The ZnO sample with 3 at% Al exhibits enhanced saturated photoconductivity under halogen lamp illumination of power 10 W/m^2. On illumination of all ZnO samples in visible light, it is found that the value of photo-generated conductivity (photoconductivity minus dark conductivity $\Delta\sigma$) is maximum for the sample ZnO:Al-2 with 3 at % of Al dopant. According to Mishra *et al.*, [13] excellent photoresponse exhibited by moderately doped samples may be due to its high conductivity at this doping concentration since on Al doping more electrons are available for charge conduction when compared to undoped ZnO samples and also as a result of lowering of barrier height at the grain boundaries in the presence of light radiation. When illumination is turned off, the decay current is found to follow the exponential relation $I_t = I_0 \exp(-t/\tau_d)$ given by equation. The fitted curves in figures display the variation of

decay time τ_d which is the time interval for the response to decay from 90% to 10% [13-15]. It is observed that Al doped samples exhibit larger decay time compared to undoped ZnO films which makes it favourable in optoelectronicapplications. The τ_d values for the samples are depicted along with the figures. The Figure. 4 (a)-(d) illustrates the behavior of both undoped and doped ZnO samples under UV irradiation that corroborates the observations from the photoconductivity under visible light. The decay constants obtained in both visible and UV radiations exhibit a close correlation in the photoresponse behavior.

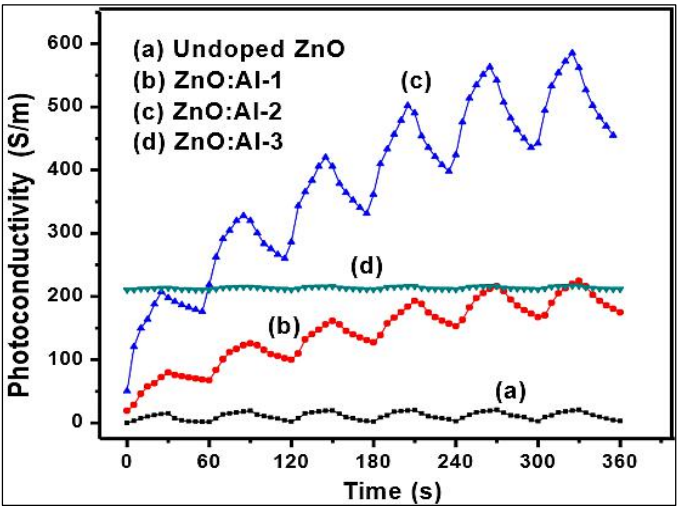

Fig 5: Transient photoresponse curves of undoped and Al doped ZnO thin films

The photoresponse of the Al doped ZnO films are checked with the time interval of 30s (Figure. 5). As can be observed from the figures the photoconductivity increases sharply when the films are illuminated by the light source and when the light is switched off, the exponential photodecay is observed similar to the behavior shown in saturated photoresponse profile. It is to be noted that as the doping concentration increases, the transient photoresponse curves move upwards after each cycle which shows that the photocurrent do not decay down to initial value after each cycle. As Moore *et al*., and Lee *et al*., [16, 17] indicate, some photoelectrons get trapped at the film surface after each cycle of time it is observed noticeably for ZnO samples that exhibit high conductivity with 1 at% and 3 at% Al content.

Table 5.1 depicts bandgap and photoresponse data of undoped and Al doped ZnO thin films and is observed that heavy doping reduces photoconductivity noticeably and similar observation has been reported

previously [9, 15]. Photosensitivity η is the ratio of photo-generated conductivity to dark conductivity $\Delta\sigma/\sigma_{dark}$ and is found to decrease with dopant concentration which obviously must be due to increase in dark conductivity.

Table 1: Optical and Photoresponse data of Undoped and Al doped ZnO thin films

Sample	Eg (eV)	σ dark (S/m)	σ_{mxm} (S/m)	Δσ (S/m)	$\eta = \Delta\sigma / \sigma_{dark}$
Undoped ZnO	3.23±0.02	0.24	31.48	31.24	128.06
ZnO: Al-1	3.27±0.01	13.56	313.33	299.77	22.11
ZnO: Al-2	3.30±0.02	61.66	601	539.34	8.75
ZnO: Al-3	3.01±0.03	210	212.83	2.83	0.013

Photoluminescence

The defect related Photoluminescence spectra of undoped and moderately doped sample ZnO:Al-2 thin films indicate (Figure. 6) the emission corresponding to near band edge (NBE) in the UV region. It is observed that Al incorporation has shifted NBE towards lower wavelength side (blue shift) when compared to undoped ZnO sample. Beegum *et al*., [18] have reported that such shift is resulted when Al^{3+} ions substitute Zn^{2+} sites of ZnO lattice causing a compressive stress. According to Ravichandran *et al*., [19] the peak at ~466nm is associated with blue emission that occurs due to transition of electron from shallow donor level of Zn interstitial to top of valence band and transition from shallow donor level of oxygen vacancies to valence band. Also, the peak at ~532nm corresponds to green emission that originates from transition between deep level ionized oxygen vacancies to valence band [20].

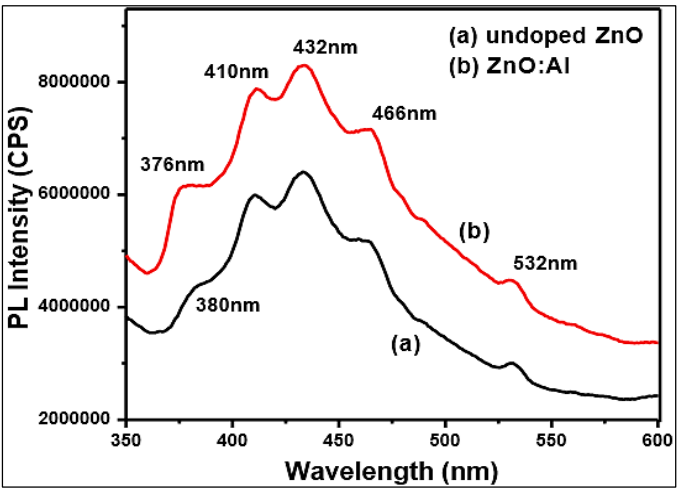

Fig 6: Photoluminescence spectrum of the sample ZnO:Al-2

ii) Optical properties of ZnO:Sn thin films

In this work, IVth group element Sn has been doped in ZnO at different concentrations. Various optical characterizations of three categories of samples with light doping of ~1 at% Sn referred to as ZnO:Sn-1, moderate doping of ~4 at% Sn named as ZnO:Sn-2 and heavy doping of ~ 9 at% Sn designated as ZnO:Sn-3 are presented.

Optical absorption and transmission

The absorbance spectra of undoped and Sn doped samples of ZnO thin filmsillustrated in Figure. 6(a) indicate gradual variation of the absorbance in the visible region (380nm-780nm) with Sn doping. Figure. 6(b) demonstrates the variation in transmittance of pure and Sn doped ZnO films which show considerably high transmittance of ~80-85% in the visible region. Even though Sn doping does not produce appreciable variation in optical bandgap, a small shift of fundamental absorption edge towards shorter wavelength is observed in the absorption spectra of all ZnO:Sn films. This suggests a slight blue shift in band gap on doping which may be due to Burstein- Moss effect. The optical energy band gap E.g. is determined from Tauc's plot as shown in Figure.7 which confirms that the films possess a direct bandgap. The optical band gapof samples slightly varies on doping from ~3.23eV in ZnO to ~3.27eV in Sn doped samples. Vishwas *et al*., [21] have observed similar variations and suggest that Sn doping increases the carrier concentration, when the Zn^{2+} ions are replaced by Sn^{4+} ions, which may shift the Fermi level [22, 23] leading to shift in bandgap and increase in optical transmittance.

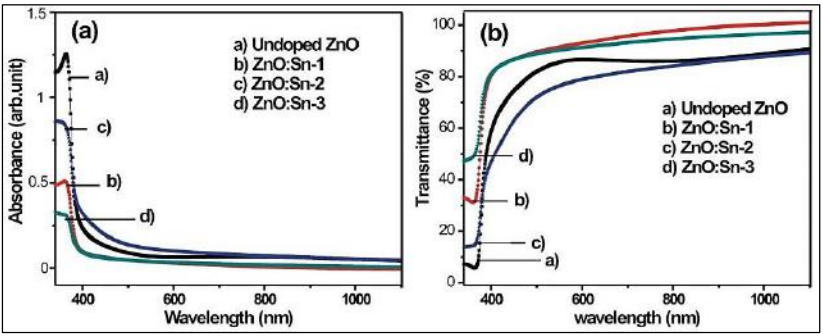

Fig 7: a) absorbance and b) Transmittance graph of undoped and Sn doped ZnOthin films

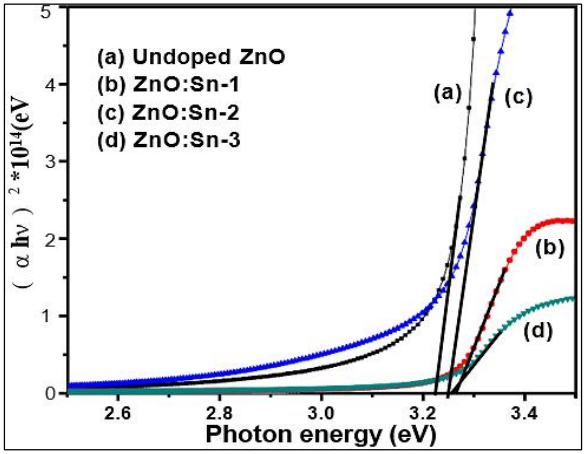

Fig 8: Tauc's plot showing optical bandgap of undoped and Sn doped ZnO samples

Optical properties of ZnO:Cu thin films

The variation in optical properties of ZnO thin films are investigated by doping the sample at different concentrations of I group element Cu which has produced noticeable variations in their optical behavior. Three categories of samples that are lightly doped (~1at% Cu), moderately doped (~4at% Cu) and heavily doped (~7at% Cu) designated as ZnO:Cu-1, ZnO:Cu-2 and ZnO:Cu-3 respectively are subjected to detailed optical characterizations.

Optical absorption and transmission analysis

Optical absorption spectra of Cu doped ZnO samples are investigated in UV-Vis range. The absorbance graph of undoped and Cu doped ZnO thin films are depicted in Figure. 9(a) where heavy doping increases absorbance. Figure 5.19(b) illustrates the transmittance graph plotted for different concentration of Cu which indicates that transmittance is affected by percentage of concentration of dopant where increase in Cu dopant leads to decrease in transparency. In transparent metal oxides, metal concentration influences the transmittance of the films. The better transmittance is shown by Cu doping at 1at% and as concentration rises to 7 at% transmittance reduces considerably.

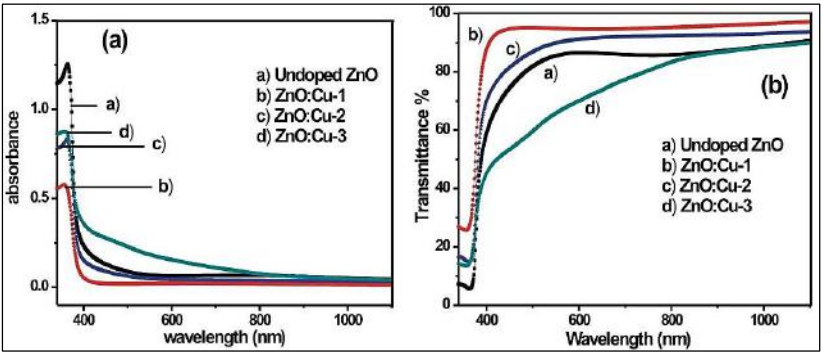

Fig 9: a) absorbance and b) Transmittance graph of undoped and Cu doped ZnOthin films

Bandgap is determined from Tauc's plot shown in Figure.10. Sung *et al*., [35] have reported a redshift in bandgap on Cu doping which is attributed to hybridization of Cu 3d bands with O 2p bands.

But in the current investigation, on light and moderate doping of Cu, a slight increase in bandgap is observed. Reports indicate similar results on Cu doping and the possible reason has been assigned to the reduction in crystallite size of the particle [36]. Here also, a decrease in crystallite size correspondingly results in blueshift of E.g. while in sample ZnO:Cu-3, at 7 at% Cu a decrease in bandgap and larger grain size are observed. The observations on optical band gap of all doped films can be directly correlated to reduction in crystallite size of the samples.

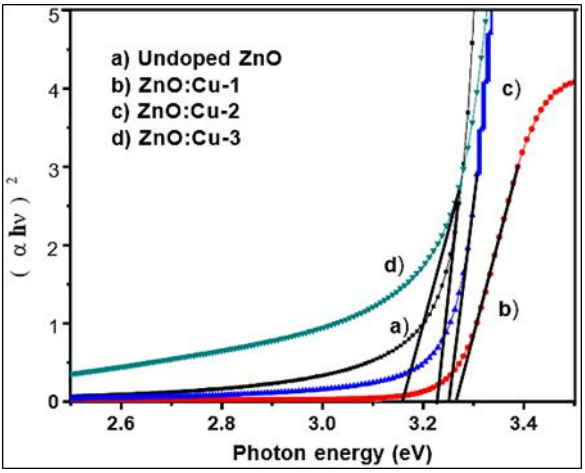

Fig 10: Tauc's plot showing bandgap of undoped and Cu doped ZnO thin films

Photo response studies

Photosensitivity measurements are done under visible light and UV radiation. The sample ZnO:Cu-2 shows very little photosensitivity and sample ZnO:Cu-3 exhibits no change in photocurrent to both white light and UV radiation while lightly doped samples respond moderately to light radiation. In this regard, it is understood that the presence of more dopant atoms enhances the probability for re-combination of electron-hole pairs that decreases the photocurrent under steady state illumination. The fitted decay curves of Cu doped samples in Figure 5.21(a)-(c) indicate no noticeable improvement in decay time τ_d compared to undoped ZnO sample. The photo-generated conductivity for Cu doped samples is less than that for undoped samples as doped samples are more resistive [4, 37, 38]. The UV conductivity profile of Cu doped ZnO samples follow the same pattern of Photo conductivity in the visible range, but the photo-generated conductivity in UV region is less intense compared to that in visible region.

The decay time constant τ_d obtained from UV conductivity studies closely correlate the data from photoconductivity in visible region.

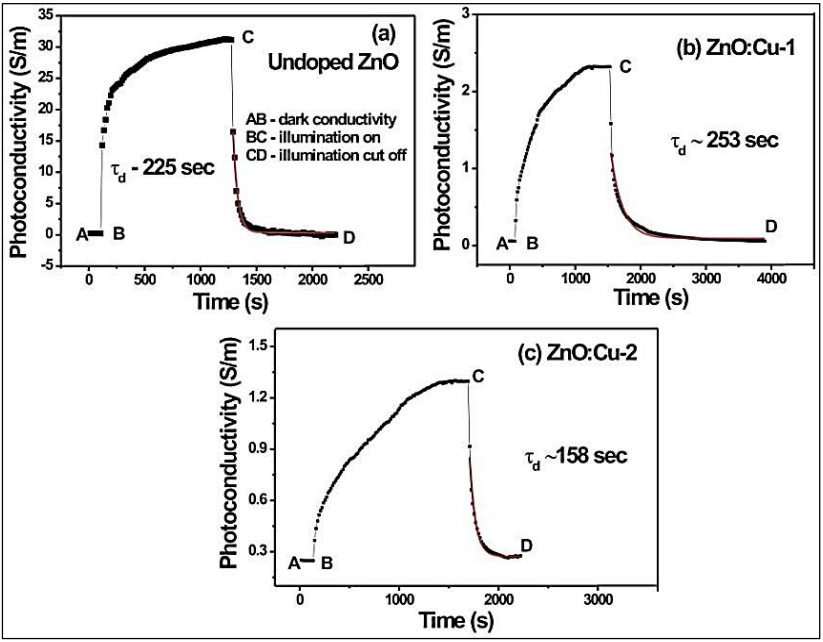

Fig 11: (a-c) Photoresponse (visible light) profile of undoped and Cu doped ZnOthin films

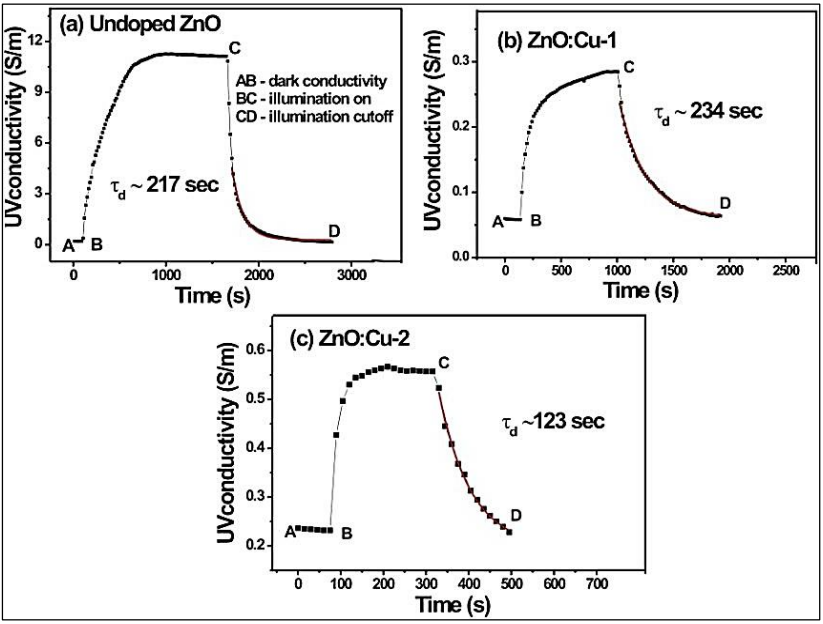

Fig 12: (a-c) UV response curves of undoped and Cu doped ZnO thin films

The transient photoresponse curve at 30s interval depicted in Figure. 13 clearly indicate the reduction in photoconductivity on doping ZnO with Cu. Many researchers have reported similar observations and suggest the poor carrier concentration as one ofthe reasons.

Moreover, being a I group element, Cu has a tendency to act as an acceptor which may affect the conductivity. The sample ZnO:Cu-3 with doping of 7 at % Cu exhibits no response to light photons both in visible and UV region of wavelength. This may be due to the presence of large number of Cu in the lattice [30, 39, 40].

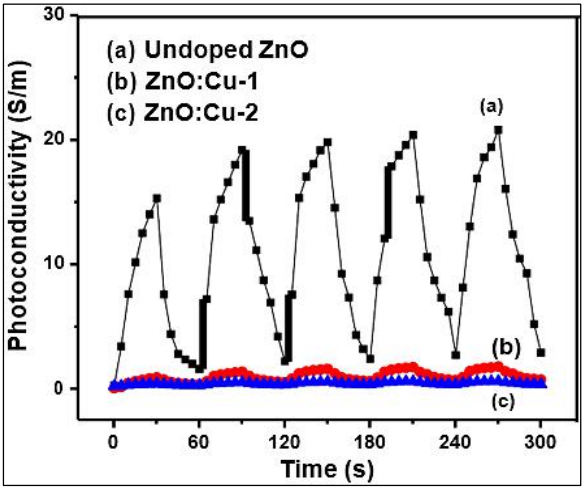

Fig 13: Transient Photo response curves of undoped and Cu doped ZnO thin films

Table 2: Optical and photo response data of undoped and Cu doped ZnO thin films

Sample	Eg (eV)	σ dark (S/m)	σmxm(S/m)	Δσ (S/m)	η =Δσ /σ_{dark}
Undoped ZnO	3.23±0.02	0.24	31.48	31.24	128.06
ZnO:Cu-1	3.27±0.02	0.062	2.325	2.263	36.5
ZnO:Cu-2	3.25±0.01	0.232	1.301	1.069	4.61
ZnO:Cu-3	3.12±0.02	-	-	-	-

Conclusion

Investigations on optical properties of ZnO thin films doped with impurities Al, Sn, Sb and Cu exhibit noticeable and systematic variations based on both doping concentration and nature of dopant. All ZnO samples uniquely exhibit improved transparency irrespective of the type of dopant. But it is noticed that among every set of doped samples, light and moderate doping produce slight shift in bandgap towards higher energy side while heavy doping reduces bandgap slightly. However, doping does not seem to produce very high variations in bandgap. Among the samples, Sb doping produces highest transparency of ~95%. Photo response studies indicate noticeable variation in photoconductivity amid different doped samples depending on variation in dopant concentrations. Photo response studies indicate that Al doped ZnO samples exhibit highest values for photo generated conductivity for light and moderate doping whileheavy doping of 10 at% Al shows a sharp decline in photo response. In addition, thesetwo samples possess improved transparency of ~90%. The combined effect of these properties make the samples ZnO:Al-1 and ZnO:Al-2 favourable in

opto-electronic applications. Comparatively higher value of photo decay constant complement the application of these samples in solar cell devices. Close behind Al samples, ZnO:Sb-3 samples also exhibit reasonably good photo-generated conductivity. In the present study, the incorporation of Cu which is an element from I group resulted in improved transparency for light and moderate doping, but photo response for the samples are observed to be low compared to undoped ZnO samples. Sn doping exhibits a systematic improvement in photoresponse with dopant concentrations. The observations from photo response in visible region are corroborated by the data obtained from UV radiation in all samples. The photo decay constants τ_d evaluated separately from visible and UV light radiation strongly correlate with each other. Photoluminescence spectral analysis has been carried out and on comparison with one sample from each dopant to undoped ZnO, all samples exhibited peaks corresponding to intrinsic defects like Zinc interstitials and Oxygen vacancy. All the doped samples show increased intensity for PL spectra except in the case of Cu doped films. But Cu doped films indicate the presence of Cu impurity which is not clearly indicated by other dopants.

Reference

1. Singh NB, Hopkins RH, Mazelsky R, Dorman HH, Mater. Lett. 1986; 4: 357-359.
2. Aoki T, Hatanaka Y, Look DC. Appl. Phys. Lett. 2000; 76:3257-3258.
3. Chen LC, Ho YC, Yang RY, Chen JH, Huang CM. Appl. Surf. Science. 2012; 258:6558-6563.
4. Kouklin N, Omari M, Gupta A. Nanowires Science and Technology, Publishers: In Tech, Croatia, 2010.
5. Tsuchiya T, Emoto T, Sei T. Journal of Non-Crystalline Solids. 1994; 178:327-332.
6. Seeber WT, Abou-Helal MO, Barth S, Beila D, Hoche T, Afify HH *et al*. Materials Science in Semiconductor Processing. 1999; 2:45-55.
7. Liu JM. Photonic Devices, Publishers: Cambridge University Press, Cambridge, New York, 2005.
8. Pisarkiewicz T. Opto-Electronics Review. 2004; 12:33-40.
9. Eskandari F, Ranjbar M, Kameli P, Salamati H. Journal of Alloys and Compounds. 2015; 649:35-45.
10. Sharma BK, Khare N. J Phys. D: Appl. Phys. 2010; 43:465-402, 1-6.
11. Caglar M, Ilican S, Caglar Y, Yakuphanoglu F. J Mater Sci: Mater Electron. 2008; 19:704-708.

12. Oh H, Krantz J, Litzov I, Stubhan T, Pinna L, Brabec CJ. Solar Energy Materials & Solar Cells. 2011; 95:2194-2199.
13. Mishra SK, Bayan S, Shankar R, Chakraborty P, Srivastava RK. Sensors and Actuators A. 2014; 211:8-14.
14. Sharma P, Mansingh A, Sreenivas K. Applied Physics Letters. 2002; 80:553-555.
15. Ganesh T, Rajesh S, Francis P. Xavier, Indian Journal of Science and Technology. 2012; 5:2360-2363.
16. Moore JC, Thompson CV. Sensors. 2013; 13:9921-9940.
17. Lee P, Chang S, Chang J, Hsu E, Chang S. Int. J Electrochem. Sci. 2013; 8:6425-6432.
18. Begum NJ, Ravichandran K. Journal of Physics and Chemistry of Solids. 2013; 74:841-848.
19. Kohan AF, Ceder G, Morgan D. Phys. Rev. 2000; D61:15019-15027
20. Pauporte T, Lincot D. Electrochimica Acta. 2000; 45:3345-3353.
21. Aksoy S, Caglar Y, Ilican S, Caglar M. Optica Applicata. 2010; 40:7-14.
22. Yung KC, Liem H, Choy HS. J Phys. D: Appl. Phys. 2009; 42:185-002, 1-5.
23. Vishwas M, Rao KN, Gowda KVA, Chakradhar RPS. Spectrochimica Acta Part A: Molecular and Biomolecular Spectroscopy. 2012; 95:423-426.
24. Mridha S, Basak D. J Phys. D: Appl. Phys. 2007; 40:6902-6907.
25. Ahn S, Ji HJ, Kim K, Kim GT, Bae CH, Park SM *et al*. Applied Physics Letters. 2007; 90:153-106, 1-6.
26. Li Y, Valle FD, Simonnet M, Yamada I. Jean-Jacques, Delaunaya, Applied Physics Letters. 2009; 94:023-110, 1-4.
27. Chow L, Lupan O, Chai G, Khallaf H, Ono LK, Roldan Cuenya B *et al*. Schulte, Sensors and Actuators A. 2013; 189:399-408.
28. Ravichandran K, Vasanthi M, Thirumurugan K, Sakthivel B, Karthika K. Optical Materials. 2014; 37:59-64.
29. Benelmadjat H, Boudine B, Halimi O, Sebais M. Optics & Laser Technology. 2009; 41:630-633.
30. Mohite SV, Rajpure KY. Optical Materials. 2014; 36:833-838.
31. Shinde VR, Gujar TP, Lokhande CD. Solar Energy Materials & Solar Cells. 2007; 91:1055-1061.

32. Panda SK, Jacob C. Solid-State Electron. 2012; 73:44-50.

33. Demirselcuk B, Bilgin V. Appl. Surf. Sci. 2013; 273:478-483.

34. Xianwen K, Fukai S, Young SP, Yunjin W, Tae WK, Fu Dejun. Surf. Coat. Tech. 2007; 201:6797-6801.

35. Sung N, Kang S, Shin H, Lee H, Lee I. Thin Solid Films. 2013; 547:285-288.

36. Jongnavakit P, Amornpitoksuk P, Suwanboon S, Ndiege N. Applied Surface Science. 2012; 258:8192-8198.

37. Li Ong W, Huang H, Xiao J, Zeng K, Ho GW. Nanoscale. 2014; 6: 1680-1690

38. Nikolai Kouklin, Adv. Mater. 2008; 20:2190-2194.

39. Pal N, Paul M, Bera A, Basak D, Bhaumik A. Analytica Chimica Acta. 2010; 674:96-101.

40. Peng L, Zhai J, Wang D, Wang P, Zhang Y, Pang S, Xie T. Chemical Physics Letters. 2008; 456:231-235.

41. Ma L, Ma S, Chen H, Ai X, Huang X. Applied Surface Science. 2011; 257:10036-10041.

Chapter - 5
Despeckling of SAR Images using Intensity Coherence Vector Segmentation

Authors

B. Mala Konda Reddy
Research Scholar, Department of ECE, KL Deemed to be University, Andhra Pradesh, India

Md. Zia Ur Rehman
Professor, KL Deemed to be University, Guntur, Andhra Pradesh, India

Chapter - 5

Despeckling of SAR Images using Intensity Coherence Vector Segmentation

B. Mala Konda Reddy and Md. Zia Ur Rehman

Abstract

Noise will be unavoidable in image acquisition practice and denoising is a necessary step to recover the image quality. Synthetic Aperture Radar (SAR) images are inherently exaggerated by speckle noise, which occur due to coherent nature of the scattering phenomena. Denoising SAR images aim at removing speckle while preserving image features such as texture, edges, and point targets. The mixtures of nonlocal grouping and transformed domain filtering have directed the modern denoising techniques. However, this approach makes a tough assumption that image patch itself provides an excellent approximation on the true parameter, which leads to bias problem predominantly under serious speckle noise. Another disadvantage is that the generally used patch pre-selection methods cannot efficiently exclude the outliers and damage the edges. In this chapter, the SAR image is injected with speckle noise and then edge based marker-controlled watershed segmentation is applied to identify the homogeneous regions in SAR image. For each region, the neighborhood pixels are identified by using Intensity Coherence Vector (ICV) and are denoised independently by using a local mean filtering. By separating coherent pixels from incoherent pixels, ICV's provide finer distinctions among blocks. Finally, the blocks are aggregated to form the denoised image. The experimental results show that the proposed method outperforms other methods such as patch-based filtering, non-local means, wavelets and classical speckle filters in terms higher signal-to-noise and edge preservation ratios comparatively.

Keywords: ICV, SAR, image processing

1. Introduction

Synthetic Aperture Radar (SAR) imaging is used in various applications such as urban planning, cartography, land cover mapping and cartography. SAR imaging systems are very useful in acquiring information under different

climatic conditions. Naturally, SAR images are disturbed from speckle noise, which degrades the performance of automatic SAR image interpretation and analysis. Hence, the SAR image analysis system starts with a preprocessing step to remove speckle noises before preceding the major steps like segmentation and classification (Ren *et al*. 2011; Chen *et al*. 2012 and Li *et al*. 2012). But at the same time, the despeckling step should not disturb other image features such as shapes, boundaries, and textures.

2. Despeckling method

As noted in literature, most of the enhancement techniques used in past research works not only denoise the SAR images, but also distort the background structure such as textures and edges. The filtering method proposed in this chapter works in two steps. It starts by dividing the SAR image into number of homogeneous regions, and for each region local mean filter is applied to denoise the SAR image. The homogeneous regions are identified by using an improved marker-controlled watershed segmentation algorithm and the coherent pixels are identified with the measure called Intensity Coherence Vector (ICV).

To overcome the problem of using fixed window size for spatial filters, it is introduced to segment the SAR images into homogenous regions by using watershed segmentation. Watershed algorithm has been accepted as an impressive segmentation method due to its multi advantages like simplicity, quickness and complete division of the image. The watershed algorithm can produce better segmentation though the image has low contrast and weak boundaries. Grau *et al*. (2004) presented a detailed study on algorithms that make use of watershed algorithm for image segmentation. The major limitation of the standard watershed algorithm is over-segmentation and is sensitive to noise. This problem can be resolved by considering the gradient magnitude image rather than taking the original grayscale image as input to watershed algorithm. However, the variations in gradient magnitude image, as well as negative impulse noise observed as a local minimum, can result in unexpected additional watershed segments. Numerous methods have been proposed to improve the watershed algorithm. The most prominent among them is the usage of region markers where certain desired local minima are selected as markers and then reconstruction is applied to fill the other minima to non-minimum hills. On the other hand, automatic marker selection is a challenging process and in most of the applications, human interaction is required to select appropriate markers. In addition, incorrect markers selection can dramatically affect the final result. The prior knowledge of shapes existed in the image improves the performance of the watershed segmentation as

demonstrated in several image segmentation approaches. But still, the major limitation in using prior shape and appearance models is the need to label training set of images and the set should contain all possible shapes. In this chapter, initially the SAR image is smoothened by using simple median filter, and the edge pixels are used as markers for watershed transformation. Thus the over-segmentation and sensitive to noise issues of watershed algorithm have been solved.

i) Watershed Segmentation

This section presents classical watershed segmentation algorithm for grayscale images by using spatial distance. The more detailed explanation of the algorithm can be referred in Roerdink & Meijster (2000). For an input image I, the lower slope, L(a), is calculated to find the neighbors for the pixel a, which is defined as

$$L(a) = \max_{b \in N(a) \cup a} \left(\frac{I(a) - I(b)}{d(a,b)} \right) \quad (1)$$

Where, N(a) is the set of neighbours of pixel a and d(a, b) is the Euclidean distance between a and b. In case of a = b, the L(a) value will be forced to be zero. Therefore, the cost for moving from pixel a to b is defined as

$$cost(a,b) = \begin{cases} L(a).\, d(a,b) & if I(a) > I(b), \\ L(a).\, d(a,b) & if I(a) < I(b), \\ \frac{1}{2}[L(a) + L(b)].\, d(a,b) & if I(a) = I(b). \end{cases} \quad (2)$$

If there exists a path p = (a_0..., a_l) from a_0 = a to a_l = b, the topographical distance along p between the two pixels a and b is expressed as

$$T^p_I(a,b) = \sum_{i=1}^{l-1} d(a_i, b_{i+1}) cost(a_i, b_{i+1})$$

T^p_I is the minimum distances among all paths linking the pixels a and b. Similarly, the catchment basin of a local minimum (m) is defined as the set of pixels which have similar topographical distances to m than any other local minimum. At the end, the set of pixels which do not belong to any catchment basin are referred to as the watershed pixels. The major limitation here is the over-segmentation.

ii) Marker controlled watershed segmentation

Meyer & Beucher (1990); Vincent & Soille (1991) initiated the solutions to over-segmentation problem by applying watershed algorithm with predefined local minimum known as markers. Generally, the edge pixels are used as markers in most of the segmentation algorithms. Although this

approach is widely used in many segmentation algorithms, the marker selection requires cautious user interaction or prior knowledge of the image structure. The random marker selection algorithms may resolve this problem, but there is a possibility of accepting a non-edge pixel as an edge or rejecting an edge pixel as non-edge one. And moreover, these edge detection algorithms may not produce connected edges. The morphological operations can also be used to join the disconnected edges. But still, the result highly depends on the selection of wider range of morphological parameters (Hamarneh & Li 2009). In the proposed method, watershed segmentation is applied with the edge image providing closed and complete boundaries for the catchment basins. Thus, the over-segmentation has been limited in the proposed watershed method.

Initially the edges of the SAR image are identified with canny operator (Jain 1989). The edges are open mostly and they do not produce closed boundaries. Here, watershed segmentation algorithm is applied with the edge image to make the edges connected and closed. Then this closed edge boundary is mapped with original grayscale SAR image. Each region is enclosed within the edges are extracted from the SAR image. Hence, the SAR image is segmented with minimum number of regions. Thus the over-segmentation behavior of watershed algorithm is resolved, and the fixed window size based enhancement is avoided. Moreover, the watershed algorithm is sensitive to noise, but the problem is ignored here as the proposed algorithm works with the edge map rather than grayscale image. Figure 4.1 illustrates the improvement in watershed segmentation as it results in minimum number of regions than the classical watershed algorithm. In the next step, Intensity Coherence Vector (ICV) is calculated at each sub-region from watershed algorithm to find the coherent pixels inside the sub region, and they are denoised with a simple filtering approach.

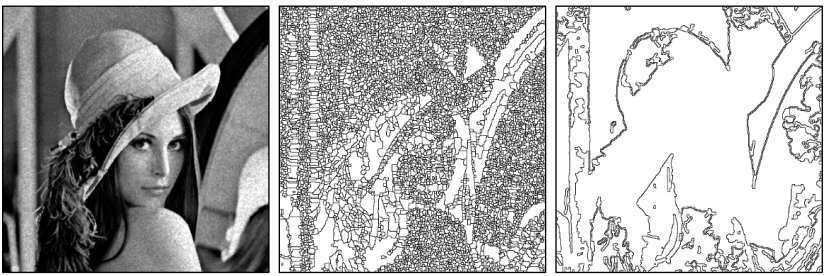

Fig 1: a) Noisy peppers image, b) Standard watershed segmentation, c) Watershed segmentation with edge markers

3. Intensity coherence vector

Intuitively, the pixel's intensity coherence is defined as the degree to which pixels of that intensity are members of large similarly-colored regions. These significant regions are referred as coherent regions, and it is observed that they are important in characterizing images. The coherence measure ICV classifies pixels as either coherent or incoherent. Coherent pixels are a part of some sizable contiguous region, while incoherent pixels are not. A color coherence vector represents this classification for each color in the image. ICV's prevent coherent pixels in one image from matching incoherent pixels in another. This allows fine distinctions that cannot be made with histograms. This property of ICV is used here to identify the local coherence pixels at every sub-region received from improved watershed segmentation algorithm. The following text explains about the computation of ICV measure.

i) Computing ICV's

The first step in computing ICV is similar to computation of a histogram. Initially the image is discretized into "nc" number of distinct intensities to eliminate the small oscillations between neighboring pixels. The next step is to classify the pixels within a given region as either coherent or incoherent. A coherent pixel is a part of a large group of pixels of the same color, while an incoherent pixel is not. The pixel group is determined by computing connected components. A connected component C is a maximum set of pixels in such a manner that for any two pixels p, p "$\in$ C, there is a path in C between p and p". Formally, a path in C is a sequence of pixels $p = p_1, p_2..., p_n = p$" such that each pixel p_i is in C and any two sequential pixels p_i, p_{i+1} are adjacent to each other. Two pixels are considered to be adjacent if one pixel is among the eight closest neighbours to the other. In other words, diagonal neighbors are included. Note that connected components are computed within a given discretized intensity bucket. This effectively segments the sub-region based on the discretized space.

Connected components can be computed in a linear time. When this is complete, each pixel will belong to exactly one connected component. Then the pixels are classified as either coherent or incoherent depending on the size of the pixels of the connected component. A pixel is coherent if the size of its connected component exceeds a fixed value "t"; Otherwise, the pixel is incoherent. For a given discretized intensity range, some of the pixels with that intensity will be coherent and some will be incoherent. Let the number of coherent pixels of the j^{th} discretized color α_j and the number of incoherent pixels β_j and the total number of pixels with that color is $\alpha_j + \beta_j$. For each

color, the pair (α_j, β_j) is computed and it is named the coherence pair for the intensity.

The intensity coherence vector for the image consists of <(α_1, β_1)…, (α_n, β_n)>. This is a vector of coherence pairs, one for each discretized intensity value. A numerical example for computing ICVs can be referred in Pass *et al*. (1997).

4. Coherence despeckling

Once the ICVs are identified for each region, the region is marked with the coherence label. Each label is meant for corresponding coherence pixels. The pixel belonging to one particular label is extracted and their intensity values are received from the original grayscale SAR image to find their mean values. The coherence label region has the minimum of 30% of pixels (Pass *et al*. 1997). Among the entire pixels, the pixels in the coherence region alone are considered for denoising,

$$\alpha_j/n_r \geq 0.3 \quad (3)$$

Where, α_j, is the number of pixels with the coherence label "j" and n_r is the total number of pixels available in the region. Then, each pixel's intensity value is replaced with the calculated mean value, which is defined as.

$$I_i(x,y) = \Sigma\, I_i(x,y)/n_r, \text{ where } I_i(x,y) \in c_i \quad (4)$$

where, c_i is the coherence labels of the region "r", $I_i(x,y)$ is the intensity values from the SAR images which have the corresponding coherence label c_i.

This procedure will be repeated for remaining coherence labels available for the current region. And the denoising is continued with the next region, till the entire image is denoised. The following algorithm summarizes the proposed despeckling algorithm.

Step 1: Read as SAR image (If it is a color image then convert it to grayscale).

Step 2: Find the edge magnitudes of the normalized SAR image by using "canny" operator.

Step 3: Apply the watershed algorithm on edge map to get closed contours.

Step 4: Discretize the image into "nc" color bins.

Step 5: Map the edge boundaries with the grayscale image to extract the segmented regions.

Step 6: For each segmented region

a) Find the Intensity Coherence Vectors and label them.

b) For each coherence label.

i) Find the local mean value.

ii) Replace all the pixels corresponding to this coherence label with the mean value.

iii) Update the pixel values in the noisy SAR image.

Step 7: Output the denoised SAR image.

The performance of the proposed filtering approach is compared with other existing denoising approaches and is described in the following section.

5. Experimental results

In this work, both simulated and real SAR images are used to analyze the performance of the proposed SAR denoising method. Initially, the speckle noise is added to the original images to degrade them. Thus, the original images are treated as the true values and are used as numerical measures to assess the performance. In this experiment, five other methods (i.e., Frost filter, PPB, LMMSE-PCA and BM3D, BNL filter algorithms) are selected to compare them with the proposed method. The selection of these methods is based on both availability of the codes and their relevance to this work.

a. Performance evaluation

Figure 2 shows the noisy synthetic images and their corresponding denoised images from various despeckling methods. Table 2 quantifies the PSNR measure on every despeckling approach at various speckle level. From the results, it is shown that the proposed method is able to achieve highest PSNR value than other existing algorithms. The observation is that the proposed method greatly outperformed LMMSE-PCA and BM3D on most noise levels which justify the proposed denoising model for ASDN. It is also observed that the performance of LMMSE-PCA is very sensitive to noise level variation in logarithmic space. As shown in Table. 1, when the noise level is lower, LMMSE-PCA achieved lower statistics than the proposed method and the same has been depicted in Figure 2. However, with the increase of noise level, LMMSE-PCA tends to achieve comparable results with the present method in terms of PSNR. LMMSE-PCA even achieved higher PSNR on image Lena when the noise level is higher, this is reasonable because LMMSE-PCA was designed for AWGN. In case the noise level is higher, the speckle noise subject to logarithmic operation which is very close to the

Gaussian white noise. Therefore, the method can achieve good results. However, when the noise level is smaller, speckle noise begins to deviate from Gaussian distribution, and its mean value is no more zero. This discrepancy between the empirical data and the model assumption may reduce the efficiency of LPG-PCA. As shown in figure 2, images by the proposed method have little artifacts but plenty of image details.

Table 1: Performance Analysis of Despeckling Methods with PSNR measure

Methods	**σ = 10**	**σ = 20**	**σ = 40**	**σ = 60**	**L = 1**	**L = 2**	**L = 4**	**L = 16**
	Lena				**Lena**			
Noisy Image	20.7587	17.1390	11.4867	7.9778	7.3898	11.027	16.7051	19.6932
ICV Filter	27.6268	20.0711	16.6610	11.2797	10.8544	16.5539	19.4281	25.0209
PPB	25.1151	19.5937	16.0637	11.0143	9.3221	16.3793	19.1292	24.6742
BNL	24.8236	19.5841	15.0280	10.5440	8.9056	15.987	18.9102	24.0532
BM3D	21.9269	19.3041	14.8819	10.2406	8.8051	15.9825	17.5855	23.437
LMMSE	21.7412	19.1026	14.5995	9.9526	8.516	13.5168	17.0804	23.2258
Frost Filter	21.0583	18.7577	13.6381	8.8053	8.0219	11.9655	16.9041	20.572
	Barbara				**Barbara**			
Noisy Image	25.7887	19.9110	13.2273	7.3121	7.1066	11.5388	17.5223	24.7811
ICV Filter	27.9905	25.4334	18.1268	12.8995	11.4685	16.4078	24.5618	27.2124
PPB	27.8136	25.2017	17.0191	12.8456	11.37	15.4094	24.5255	27.0905
BNL	27.4457	24.9676	15.4558	9.5269	8.9546	14.7728	24.3604	27.029
BM3D	27.2071	23.9254	14.4024	9.2818	8.7224	13.8627	24.0267	26.7748
LMMSE	26.9410	23.4002	14.3659	8.3967	8.6743	13.6512	23.1624	26.7715
Frost Filter	26.7044	22.6765	14.1474	8.2322	7.755	11.8608	18.762	24.8376
	Peppers				**Peppers**			
Noisy Image	23.8752	20.8165	14.7640	7.0622	8.1508	11.2913	14.3378	19.003
ICV Filter	27.5116	22.9032	17.4026	14.5931	10.2208	14.1369	17.6345	27.3188
PPB	27.0170	22.6405	17.0358	12.6966	9.386	13.7977	17.1735	23.3213
BNL	25.7285	21.9789	16.7817	10.1972	8.8878	13.5895	16.5519	22.935
BM3D	25.0391	21.6603	15.8126	9.8881	8.8658	13.2849	16.3338	21.2592

Figure. 2 illustrates the sample outputs from the proposed despeckling and five other existing methods with synthetic images at noise variance 10 with 16 multiple looks.

Lena

(a) **(b)** **(c)**

(d) **(e)** **(f)** **(g)**

Barbara

(a) **(b)** **(c)**

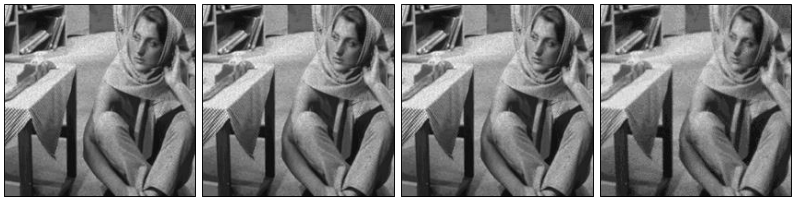

(d) **(e)** **(f)** **(g)**

Boats

(a) **(b)** **(c)**

(d) **(e)** **(f)** **(g)**

Lake

(a) **(b)** **(c)**

(d) **(e)** **(f)** **(g)**

Fig 2: Denoised output from despeckling methods with synthetic images (σ=10, L=16). (a) Noisy image, (b) ICV filter, (c) PPB, (d). BNL, (e) BM3D, (f) LMMSE and (g) Frost Filter Results

Table. 2 depicts the SCR values received from despeckling methods. Again, the proposed method outperforms other methods by attaining highest SCR value than others for all synthetic images.

Table 2: Performance Analysis of Despeckling Methods with SCR measure

Methods	**σ = 10**	**σ = 20**	**σ = 40**	**σ = 60**	**L = 1**	**L = 2**	**L = 4**	**L = 16**
	Lena				**Lena**			
Noisy Image	3.4991	3.1748	2.6596	2.4265	2.4195	2.5855	2.9135	3.1671
ICV Filter	3.7693	3.4900	3.1115	2.6014	2.5757	2.8127	3.1197	3.7660
PPB	3.7658	3.4512	3.0831	2.5663	2.5548	2.7844	3.0869	3.6444
BNL	3.6302	3.3669	3.0612	2.5573	2.5128	2.7411	3.0487	3.3506
BM3D	3.6277	3.3424	2.9463	2.4872	2.4853	2.7251	3.0392	3.2992

LMMSE	3.5954	3.3085	2.9012	2.4693	2.4438	2.6912	2.9558	3.2410
Frost Filter	3.5698	3.1912	2.8066	2.4388	2.4351	2.6303	2.9488	3.1736
	Barbara				**Barbara**			
Noisy Image	3.4028	2.9515	2.6450	2.4236	2.4006	2.7118	3.1700	3.5332
ICV Filter	3.7414	3.1390	2.9362	2.6216	2.6784	3.1310	3.5102	3.7622

Table 2: Continued

PPB	3.6931	3.1387	2.9048	2.6109	2.6145	3.0572	3.4071	3.7098
BNL	3.6666	3.1179	2.8788	2.6024	2.5558	3.0122	3.3639	3.6519
BM3D	3.6269	3.0138	2.7634	2.5898	2.4628	2.9165	3.3224	3.6329
LMMSE	3.5536	2.9940	2.7593	2.5682	2.4624	2.8956	3.2892	3.5733
Frost Filter	3.4825	2.9851	2.7491	2.4767	2.4566	2.8408	3.1786	3.5383
Methods	**σ = 10**	**σ = 20**	**σ = 40**	**σ = 60**	**L = 1**	**L = 2**	**L = 4**	**L = 16**
	Peppers				**Peppers**			
Noisy Image	3.5644	3.1566	2.8407	2.4143	2.5103	2.8761	3.2417	3.4062
ICV Filter	3.7616	3.4841	3.1353	2.6177	2.8544	3.2243	3.3563	3.7203
PPB	3.6761	3.4503	3.0962	2.6052	2.7748	3.0754	3.3157	3.6948
BNL	3.6605	3.3998	3.0817	2.5670	2.6843	3.0052	3.2898	3.6696
BM3D	3.6507	3.3836	3.0366	2.5077	2.6705	3.0017	3.2816	3.6672
LMMSE	3.6332	3.1903	3.0175	2.4720	2.5319	2.9070	3.2647	3.5986
Frost Filter	3.5780	3.1896	3.0023	2.4390	2.5270	2.8824	3.2424	3.5468
	Boats				**Boats**			
Noisy Image	3.4093	3.3345	3.0587	2.5204	2.4589	3.0561	3.3334	3.5967
ICV Filter	3.7748	3.3755	3.2092	2.9498	2.8368	3.2518	3.5859	3.7837
PPB	3.6751	3.3628	3.1955	2.8967	2.8198	3.2315	3.5417	3.7092
BNL	3.6699	3.3516	3.1824	2.7663	2.7365	3.1365	3.4644	3.6912
BM3D	3.4928	3.3422	3.1000	2.6725	2.6942	3.1364	3.3972	3.6835
LMMSE	3.4400	3.3417	3.0944	2.6268	2.6384	3.1033	3.3578	3.6693
Frost Filter	3.4327	3.3396	3.0699	2.6162	2.5506	3.0619	3.3512	3.6385

Table. 3 shows the values of β measure calculated for each denoising methods. The greater value of the proposed method states that this algorithm can preserve the edges better than any other method.

Table 3: Performance Analysis of Despeckling Methods with β measure

Methods	**σ = 10**	**σ = 20**	**σ = 40**	**σ = 60**	**L = 1**	**L = 2**	**L = 4**	**L = 16**
	Lena				**Lena**			
Noisy Image	0.8906	0.7787	0.6685	0.6005	0.6405	0.7162	0.7962	0.9147
ICV	0.9595	0.8555	0.7778	0.6683	0.7048	0.7869	0.9082	0.9799

Filter								
PPB	0.9569	0.8403	0.7556	0.6658	0.6820	0.7695	0.8998	0.9724
BNL	0.9479	0.8168	0.7455	0.6475	0.6781	0.7562	0.8877	0.9539
BM3D	0.9185	0.8058	0.7074	0.6459	0.6741	0.7531	0.8864	0.9253
LMMSE	0.9171	0.7882	0.6910	0.6361	0.6741	0.7199	0.8455	0.9214
Frost Filter	0.8998	0.7820	0.6785	0.6164	0.6482	0.7176	0.8119	0.9195
	Barbara				**Barbara**			
Noisy Image	0.8369	0.7524	0.6673	0.6055	0.6126	0.7662	0.8703	0.9444
ICV Filter	0.9709	0.8253	0.7486	0.6614	0.7438	0.8675	0.9410	0.9699
PPB	0.9283	0.8099	0.7291	0.6527	0.7353	0.8376	0.9399	0.9596
BNL	0.8699	0.7931	0.7230	0.6517	0.7222	0.8309	0.9292	0.9566
BM3D	0.8539	0.7913	0.6773	0.6344	0.7069	0.8259	0.9256	0.9561
LMMSE	0.8475	0.7859	0.6754	0.6317	0.6786	0.8135	0.9232	0.9551
Frost Filter	0.8472	0.7634	0.6690	0.6182	0.6609	0.8062	0.8731	0.9542
	Peppers				**Peppers**			
Noisy Image	0.9236	0.8237	0.7038	0.6201	0.6013	0.7092	0.7937	0.8914

Table 3: Continued

ICV Filter	0.9653	0.9138	0.8170	0.6973	0.7058	0.7754	0.8750	0.9772
Methods	**σ = 10**	**σ = 20**	**σ = 40**	**σ = 60**	**L = 1**	**L = 2**	**L = 4**	**L = 16**
PPB	0.9621	0.9088	0.8111	0.6932	0.7051	0.7492	0.8602	0.9753
BNL	0.9418	0.9085	0.7936	0.6926	0.7027	0.7245	0.8540	0.9373
BM3D	0.9375	0.8679	0.7927	0.6860	0.6919	0.7179	0.8519	0.9229
LMMSE	0.9353	0.8413	0.7294	0.6858	0.6796	0.7135	0.8509	0.9125
Frost Filter	0.9347	0.8367	0.7262	0.6741	0.6504	0.7134	0.8460	0.9078
	Boats				**Boats**			
Noisy Image	0.9045	0.8232	0.7259	0.6104	0.6075	0.6574	0.7572	0.8881
ICV Filter	0.9713	0.8988	0.8223	0.7249	0.6506	0.7445	0.8864	0.9665
PPB	0.9673	0.8813	0.8140	0.7240	0.6486	0.7261	0.8853	0.9452
BNL	0.9440	0.8569	0.8006	0.7195	0.6412	0.7189	0.8713	0.9371
BM3D	0.9351	0.8508	0.7551	0.6668	0.6323	0.6964	0.8095	0.9336
LMMSE	0.9334	0.8339	0.7510	0.6508	0.6187	0.6909	0.7997	0.9177
Frost Filter	0.9212	0.8234	0.7494	0.6231	0.6168	0.6902	0.7943	0.9176

Table 4.4 presents the second measure (EPI) values of each denoising methods. The closer value to one for the proposed method states that this algorithm can preserve edges better than any other methods.

Table 4: Performance Analysis of Despeckling Methods with EPI measure

Methods	σ = 10	σ = 20	σ = 40	σ = 60	L = 1	L = 2	L = 4	L = 16
	Lena				**Lena**			
Noisy Image	0.7561	0.6818	0.6122	0.4833	0.4517	0.5189	0.5908	0.6532
ICV	0.8305	0.7479	0.6807	0.5967	0.5021	0.5826	0.6518	0.8332
PPB	0.8072	0.7386	0.6729	0.5769	0.4792	0.5816	0.6514	0.8087
BNL	0.8052	0.7127	0.6590	0.5516	0.4763	0.5728	0.6298	0.7937
BM3D	0.7967	0.7098	0.6589	0.5321	0.4747	0.5662	0.6254	0.7862
LMMSE	0.7900	0.6864	0.6569	0.5222	0.4708	0.5660	0.6159	0.7817
Frost	0.7783	0.6833	0.6324	0.5174	0.4661	0.5399	0.6034	0.7146
	Barbara				**Barbara**			
Noisy Image	0.7126	0.6050	0.5417	0.4501	0.4741	0.5899	0.6347	0.7241
ICV	0.8454	0.7057	0.5952	0.5360	0.5836	0.6241	0.7237	0.8363
PPB	0.8385	0.7014	0.5799	0.5029	0.5822	0.6164	0.7165	0.7724
BNL	0.7801	0.6898	0.5789	0.4957	0.5546	0.6121	0.7125	0.7635
BM3D	0.7498	0.6676	0.5733	0.4874	0.5105	0.6085	0.7040	0.7524
LMMSE	0.7310	0.6560	0.5548	0.4859	0.4982	0.5998	0.6511	0.7426
Frost	0.7230	0.6308	0.5447	0.4564	0.4946	0.5949	0.6414	0.7393
	Peppers				**Peppers**			
Noisy Image	0.7802	0.5871	0.5054	0.4535	0.4549	0.5516	0.6655	0.7584
ICV	0.8486	0.7798	0.5824	0.5042	0.5481	0.6592	0.7481	0.8401
PPB	0.8413	0.6856	0.5451	0.4948	0.5001	0.6413	0.7453	0.8220
BNL	0.8401	0.6850	0.5331	0.4828	0.4901	0.6386	0.7348	0.8148
BM3D	0.8265	0.6489	0.5265	0.4542	0.4714	0.5728	0.7345	0.8082
LMMSE	0.8181	0.6334	0.5181	0.4538	0.4624	0.5601	0.7050	0.8008
Frost	0.8069	0.6134	0.5164	0.4537	0.4579	0.5533	0.7035	0.7654

Table 4: Continued

Methods	σ = 10	σ = 20	σ = 40	σ = 60	L = 1	L = 2	L = 4	L = 16
	Boats				**Boats**			
Noisy Image	0.7574	0.7107	0.5932	0.4817	0.4726	0.5448	0.5938	0.6653
ICV Filter	0.8245	0.7458	0.7098	0.5787	0.5354	0.5827	0.6568	0.8188
PPB	0.8137	0.7333	0.7019	0.5264	0.4931	0.5819	0.6460	0.7834
BNL	0.8060	0.7323	0.7004	0.5252	0.4914	0.5719	0.6333	0.7577
BM3D	0.7945	0.7311	0.6902	0.4969	0.4887	0.5678	0.6145	0.7533
LMMSE	0.7821	0.7230	0.6792	0.4944	0.4872	0.5607	0.6078	0.7067
Frost	0.7637	0.7202	0.6028	0.4941	0.4855	0.5488	0.5944	0.6906

The average performance of the proposed Despeckling method on synthetic images is analyzed with the noise variance 10 and 20, number of

looks 2 and 4. The ICV filter based denoising is applied on synthetic images 20 times at different combinations of noise variance and looks. The ANOVA test is performed to analyze the significance of noise variance and the number of looks. Figures. 3-6 depict the performance comparisons.

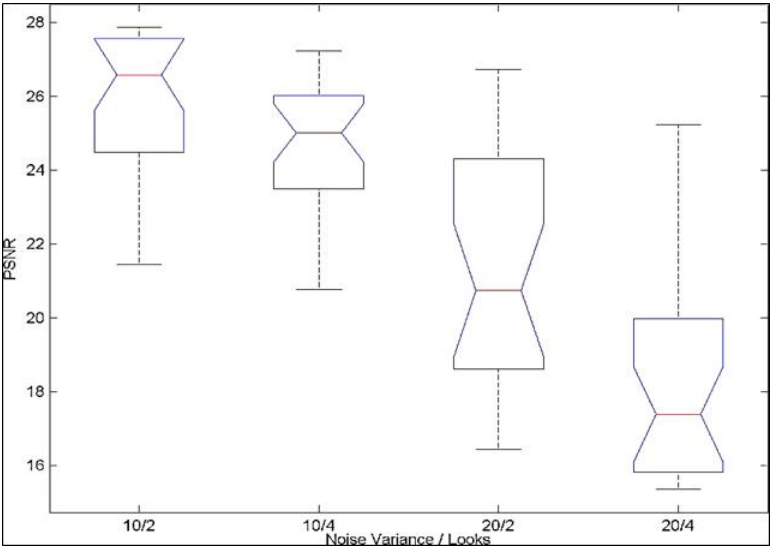

Fig 4.3: Denoising Performance of ICV filter on PSNR measure

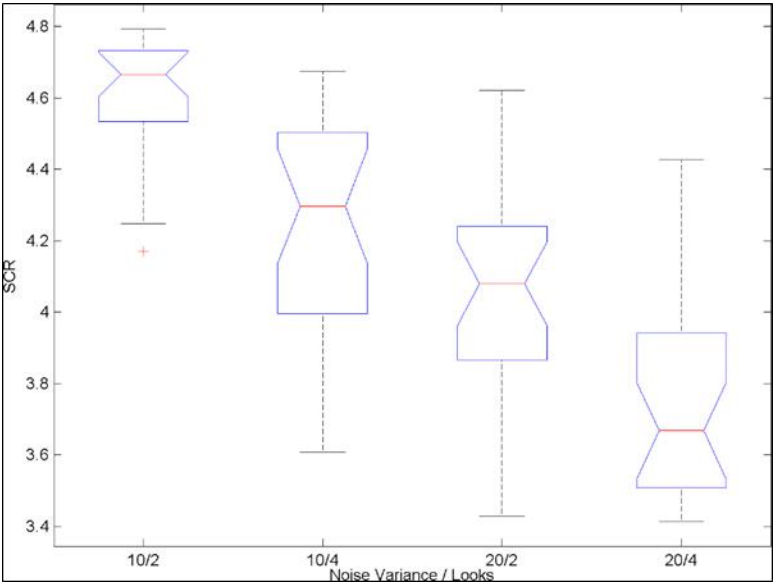

Fig 4: Denoising Performance of ICV filter on SCR measure

The summarized ANOVA statistics is depicted in Table. 5. The higher F value and the lower P value represent the noise variance and the number of looks cause significant changes on denoising performances for almost all the parameters.

Table 5: ANOVA statistics for the performance of ICV filter

Performance measure	F Statistics	P Value
PSNR	48.8709	2.90e-19
SCR	51.5377	6.18e-20
β-value	34.8776	2.47e-15
EPI	56.5709	3.78e-21

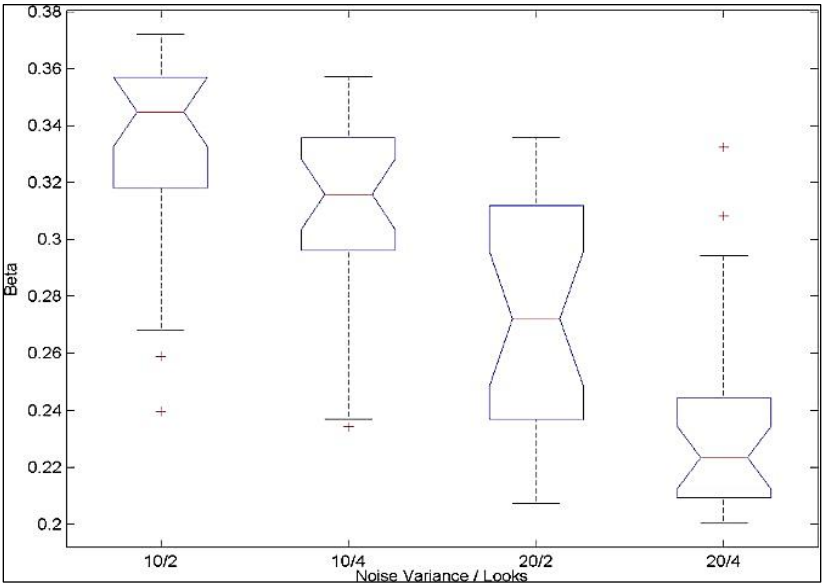

Fig 5: Denoising Performance of ICV filter on β measure

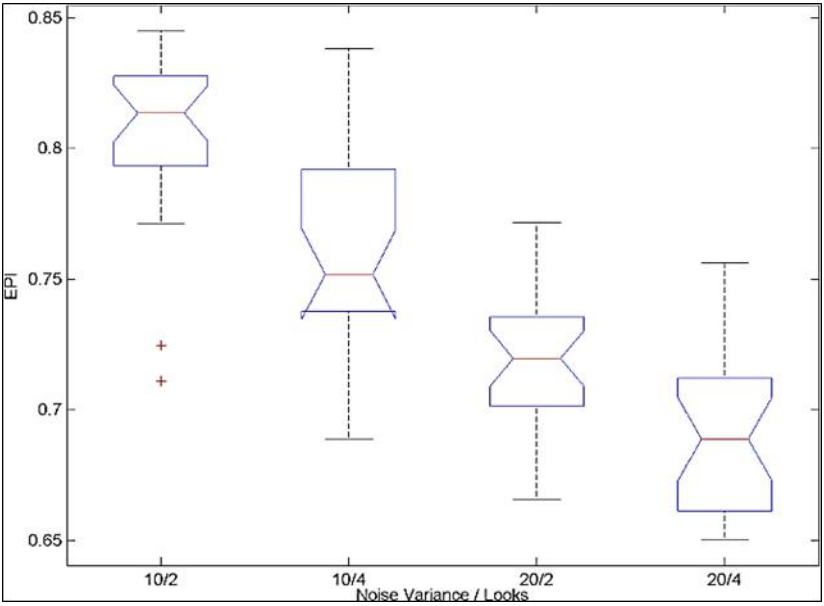

Fig 6: Denoising Performance of ICV filter on EPI measure

Table. 5 &. 6 depicts the HD and TP performance measure to compare the despeckling results from the proposed ICV filter against other filters.

Table 5: Performance Analysis of Despeckling Methods with HD measure

Methods	**σ = 10**	**σ = 20**	**σ = 40**	**σ = 60**	**L = 1**	**L = 2**	**L = 4**	**L = 16**
	Lena				**Lena**			
ICV	0.1331	0.2144	0.1775	0.3336	0.3321	0.1364	0.0750	0.0334
PPB	0.0915	0.2639	0.2736	0.3729	0.3085	0.1483	0.1800	0.0481
BNL	0.1396	0.2315	0.3136	0.3572	0.3071	0.2038	0.1280	0.0651
BM3D	0.1253	0.2550	0.2833	0.4009	0.3936	0.2206	0.1500	0.1410
LMMSE	0.1459	0.2481	0.2932	0.3577	0.3779	0.1788	0.1695	0.0741
Frost	0.2027	0.2945	0.2647	0.3715	0.4153	0.2152	0.1684	0.0870
	Barbara				**Barbara**			
ICV	0.0654	0.2908	0.1811	0.4052	0.2919	0.2207	0.1278	0.0167
PPB	0.1307	0.2181	0.2657	0.3691	0.3128	0.1703	0.1182	0.0359
BNL	0.1208	0.2816	0.2662	0.3285	0.3165	0.2312	0.1966	0.0505
BM3D	0.1053	0.2303	0.2607	0.4066	0.4259	0.1660	0.1503	0.1571
LMMSE	0.1045	0.2248	0.2706	0.3840	0.4350	0.2341	0.1453	0.1567
Frost	0.1928	0.2772	0.2543	0.4359	0.4789	0.2643	0.1827	0.1157
	Peppers				**Peppers**			
ICV	0.0634	0.2061	0.2697	0.3585	0.3232	0.1756	0.1263	0.1079

PPB	0.0827	0.2047	0.2258	0.3297	0.3738	0.1909	0.1702	0.0442
BNL	0.1318	0.2256	0.2327	0.3471	0.3312	0.1893	0.1168	0.1104
BM3D	0.1669	0.2753	0.2619	0.3953	0.4035	0.1633	0.2067	0.1429
LMMSE	0.1887	0.3087	0.2647	0.4296	0.4135	0.1694	0.1865	0.1159
Frost	0.1909	0.3084	0.2696	0.4343	0.4550	0.2404	0.1811	0.0715
	Boats				**Boats**			
ICV	0.1029	0.2040	0.2169	0.3665	0.3135	0.2030	0.0678	0.0742
PPB	0.1380	0.2008	0.2711	0.3977	0.3774	0.1456	0.1494	0.0333
BNL	0.0953	0.2292	0.2531	0.4129	0.3330	0.1943	0.1690	0.0843
BM3D	0.1591	0.2195	0.2756	0.4184	0.3927	0.1755	0.1813	0.1298
LMMSE	0.1457	0.2764	0.2768	0.3943	0.4334	0.2268	0.1592	0.1578
Frost	0.1888	0.3236	0.3119	0.4356	0.4194	0.2441	0.2313	0.0722

Table 6: Performance Analysis of Despeckling Methods with TP measure

Methods	**σ = 10**	**σ = 20**	**σ = 40**	**σ = 60**	**L = 1**	**L = 2**	**L = 4**	**L = 16**
	Lena				**Lena**			
ICV	0.9960	0.8865	0.9387	0.7484	0.7303	0.8234	0.8955	0.9717
PPB	0.9831	0.8862	0.8857	0.7498	0.6693	0.8111	0.8469	0.9606
BNL	0.9794	0.8704	0.8868	0.7417	0.6697	0.7462	0.8034	0.9599
BM3D	0.9742	0.8809	0.8395	0.7291	0.6906	0.7608	0.7982	0.9426
LMMSE	0.9772	0.8815	0.8548	0.7039	0.6579	0.7432	0.7948	0.9295
Frost	0.9636	0.8743	0.8115	0.6646	0.6765	0.7159	0.7756	0.9404
	Barbara				**Barbara**			
ICV	0.9888	0.9167	0.9140	0.7643	0.7313	0.7930	0.8514	0.9856
PPB	0.9807	0.8625	0.8923	0.7410	0.7087	0.8104	0.8158	0.9402
BNL	0.9781	0.8545	0.8953	0.7083	0.7124	0.7862	0.8043	0.9599
BM3D	0.9533	0.8832	0.8544	0.7080	0.7054	0.7399	0.7892	0.9188
LMMSE	0.9434	0.8676	0.8572	0.7155	0.6591	0.7252	0.7680	0.9593
Frost	0.9232	0.8830	0.8235	0.7085	0.6586	0.7208	0.7697	0.9434
	Peppers				**Peppers**			
ICV	0.9714	0.8870	0.9038	0.7606	0.6953	0.8034	0.8589	0.9775
PPB	0.9945	0.8679	0.9035	0.7608	0.6820	0.8157	0.8458	0.9488
BNL	1.0037	0.8899	0.8702	0.7273	0.6724	0.7475	0.7997	0.9584
BM3D	0.9863	0.8906	0.8541	0.7176	0.7068	0.7679	0.7884	0.9624
LMMSE	0.9793	0.8457	0.8391	0.7080	0.6998	0.7529	0.7843	0.9477
Frost	0.9313	0.8570	0.8073	0.6822	0.6693	0.7051	0.7793	0.9495
	Boats				**Boats**			
ICV	0.9831	0.8894	0.9252	0.7461	0.7245	0.8339	0.8614	0.9860

PPB	0.9896	0.9045	0.9147	0.7832	0.6819	0.7826	0.8206	0.9492
BNL	0.9880	0.8690	0.9072	0.7268	0.6939	0.7834	0.8038	0.9598
BM3D	0.9721	0.8937	0.8787	0.6863	0.7047	0.7581	0.7742	0.9541
LMMSE	0.9664	0.8906	0.8472	0.6839	0.6823	0.7469	0.8009	0.9486
Frost	0.9485	0.8688	0.8142	0.6689	0.6900	0.7207	0.7870	0.9418

Figure. 7 illustrates the sample output of proposed and the existing despeckling with real SAR image at the maximum of 4 different looks.

ALOS-PALSAR

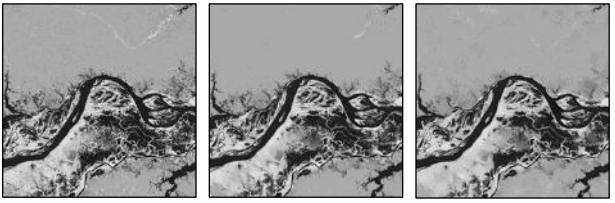

(a) **(b)** **(c)**

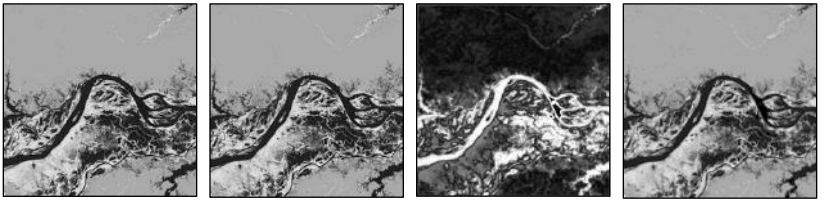

(d) **(e)** **(f)** **(g)**

Sentinel-1

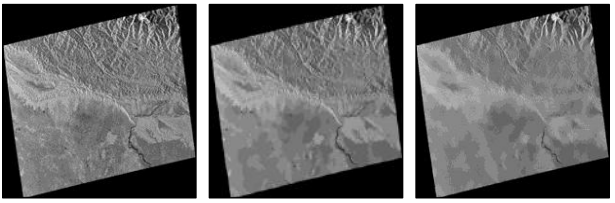

(a) **(b)** **(c)**

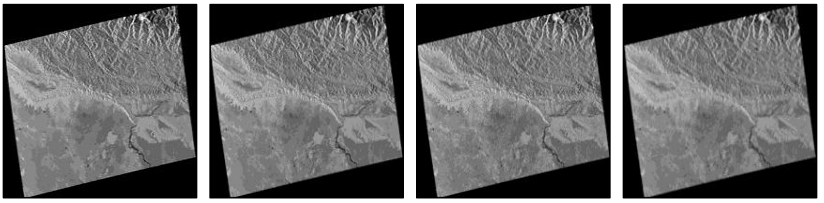

(d) **(e)** **(f)** **(g)**

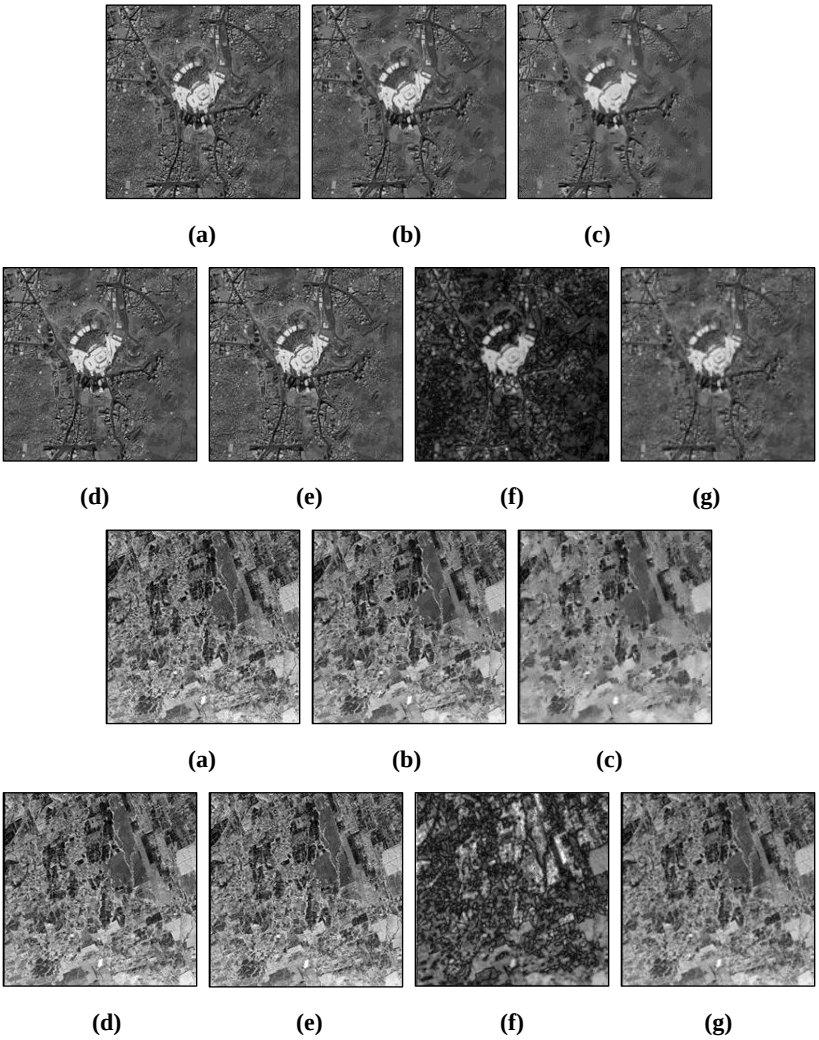

Fig 7: Denoised output from despeckling methods with real SAR images (L=4). (a) Noisy image, (b) ICV filter, (c) PPB, (d) BNL, (e) BM3D, (f) LMMSE and (g) Frost filter results

Conclusion

In this work, an SAR image despeckling scheme is proposed based on coherence structure-based segmentation with local mean filtering. Initially, watershed algorithm is applied with the edge image to receive homogeneous regions from the SAR image for each region. The coherent pixels are identified by using Intensity Coherence Vector (ICV) measure and are applied with local mean filtering. And these patches are merged together to form a

complete denoised image. Hence, the proposed approach does not make use of any fixed window size. It considers the coherence pixels for denoising through ICV and edge marker-based segmentation as well as it preserves the boundaries. The proposed denoising scheme is tested on both synthetic and real SAR images and is compared with several other state-of-the-art methods. The results demonstrate that the proposed method is comparatively better than referenced methods both in terms of image detail preservation and speckle noise reduction.

References

1. Achim A, Tsakalides P, Bezerianos A. SAR image denoising via Bayesian wavelet shrinkage based on heavy-tailed modeling, IEEE Transactions on Geoscience and Remote Sensing. 2003; 41(8):1773-1784.
2. Akansu AN, Haddad RA. Multiresolution Signal Decomposition Transforms, Subbands and Wavelets, Academic Press, New York, 1991.
3. Al Azzawi NA, Mat Sakim HA, Wan Abdhulla AK. MR image monomodal registration based on the non-subsampled contourlet transform and mutual information, International conference on Computer Applications and Industrial Electronics, 2010.
4. Ali SM, Javed MY, Khattak NS. Wavelet-based despeckling of synthetic aperture radar images using adaptive and mean filters, Proceedings of World Academy of Science, Engineering and Technology, Venice (Italy). 2010; 25:39-43.
5. Amirmazlaghani M, Amindavar H. Two novel Bayesian multiscale approaches for speckle suppression in SAR images, IEEE transaction in Geoscience and Remote Sensing. 2010; 48(7):2980-2993.
6. Argenti F, Alparone L. Speckle removal from SAR images in the undecimated wavelet domain, IEEE Transactions on Geoscience and Remote Sensing. 2002; 40(11):2363-2374.
7. Argenti F, Bianchi T, Alparone L. Multiresolution MAP despeckling of SAR images based on locally adaptive generalized Gaussian pdf modeling IEEE Transaction sons on Image Processing. 2006; 15(11):3385-3399.
8. Argenti F, Bianchi T, Lapini A, Alparone L. Fast MAP despeckling based on Laplacian-Gaussian modeling of wavelet coefficients, IEEE Geoscience and Remote Sensing Letters. 2012; 9(1):13-17.

9. Astola J, Kuosmanen P. Fundamentals of Non-linear filtering, Boca Raton (USA), CRC Press, 1997.
10. Balz T, Haala N. Interpretation of high-resolution SAR data using existing GIS data in urban areas, 2005.

Chapter - 6
Data Pre-Processing Based on Sentiment Analysis

Authors

Kolli Srikanth
Assistant Professor, IT Department, University College of Engineering, JNTUKUCEV, Vizianagaram, Andhra Pradesh, India

N.V.E.S. Murthy
Department of Mathematics, Andhra University, Visakhapatnam, Andhra Pradesh, India

P.V.G.D. Prasad Reddy
Department of Computer Science and Systems Engineering, Andhra University, Visakhapatnam, Andhra Pradesh, India

Chapter - 6

Data Pre-Processing Based on Sentiment Analysis

Kolli Srikanth, N.V.E.S. Murthy and P.V.G.D. Prasad Reddy

Abstract

A wide range of approaches to sentiment analysis on Twitter, and other similar microblogging platforms, have been recently built. Most of these approaches rely mainly on the presence of affect words or syntactic structures that explicitly and unambiguously reflect sentiment (e.g., "great", "terrible"). However, these approaches are semantically weak, that is, they do not account for the semantics of words when detecting their sentiment in text. This is problematic since the sentiment of words, in many cases, is associated with their semantics, either along the context they occur within (e.g., "great" is negative in the context "pain") or the conceptual meaning associated with the words (e.g., "Bookworm" is negative when its associated semantic concept is "Worm"). The findings from this body of work demonstrate the value of using semantics in sentiment analysis on Twitter. The proposed approaches, which consider word's semantics for sentiment analysis at both, entity and tweet levels, surpass non- semantic approaches in most datasets.

Keywords: twitter, frame work, sentiment analysis

I. Introduction

The emergence of microblogging services and social media platforms have given web users a place for expressing and sharing their thoughts and opinions on all kinds of events and topics. Social media platforms and, in particular, microblogging services such as Twitter, Tumblr, Plurk, Twister and Weibo are increasingly being adopted by users to access and show their opinion regarding a big pool of subjects. These new mediums of expression enable people to connect to each other, and voice their opinion in a simple manner [1]. Twitter, with about 650 million users and over 500 million messages per day, has become a popular social data provider for organizations to analyse their image and trademark by extracting the tweets posted by the users and customers about their services and

products. This new phenomenon has been a motivation for more research efforts, where natural language processing, information retrieval and text processing techniques are utilised to build models and approaches to analyse and track sentiment on Twitter and other similar microblogging services such as Tumbler, Plurk, Twister. Sentiment analysis or opinion mining refers to the application of techniques from fields such as natural language processing (NLP), information retrieval (IR) and machine learning (ML), to extract and identify the subjective information from text-based datasets [2]. One of the most popular sentiment analysis tasks is the automatic classification of documents or sentences into sentiment categories such as positive, negative, and neutral. These sentiment classes represent the writer's sentiment towards the topic addressed in the message. Sentiment analysis applied to social media platforms has received increasing interest from the research community due to its importance in a wide range of fields such as business, elections, politics and sports etc. Several works claim that social phenomena such as stock prices, movie box-office revenues and results in political elections, are influenced by social media data [3, 4, 5] and opinions expressed in these platforms can be used to measure the public opinion through indirect means [6].

However, relying only on the affect of words is often insufficient, and in many cases does not lead to satisfactory results.

Common examples of such cases occur when the sentiment of words differs according to

i) The context in which those words occur (e.g., "great" is negative in the context "disaster" and positive in the context "work").

ii) The conceptual meaning associated with the words (e.g., "Bookworm" is likely to be negative when its associated concept is "Worm" and likely to be neutral when its associated concept is "Study").

By ignoring the semantics of words for calculating their emotion or sentiment may give inaccurate results. Twitter has been used as a representative case study of microblogging services in the experimental work conducted in this thesis. Specifically, focus on the impact of both types of semantics in multiple sentiment analysis tasks on Twitter. This includes: entity-level sentiment analysis, i.e., detecting the sentiment of individual named-entities (e.g., "Demonetization", "Narendra Modi", etc.), and tweet-level sentiment analysis, i.e., detecting the overall sentiment of a given tweet. In this work, the main focus is on the use of semantics for

context-based sentiment lexicon adaptation, i.e., amending the prior sentiment orientation of words in general purpose sentiment lexicons with regards to the word's semantics in the context as they occur.

II. Sentiment analysis

Nowadays, study has increasingly focused on semantic analysis as a process that extracts sentiment information that is different from syntactic, semantic or statistical information. Specifically, semantic analysis deals with the extraction of user's thought, opinion and emotion extraction over different discussion forum, blogs, social sites, etc. people's interaction and curiosity towards social media and internet, have attracted many researchers to explore the user's behavioural pattern towards a specific topic. There are three levels of Sentiment analysis classifications, namely Document Level, Sentence Level and Aspect level. Document level classification done on the whole corpus of tweets and categorize them as Positive, Negative or Neutral. Pang & Lee [7, 8] classified documents not on the basis of topic, but by overall sentiment to determine whether a document is Positive or Negative. Sentence level classification considers a tweet as a sentence and calculates the sentiment related to the sentence. The aspect/feature level provides a more fine-grained model in which sentiments or opinions can be extracted from different aspects or features of the entity. In this level, opinions or sentiments are extracted and assigned them a related class by determining the polarity to conclude the result. Fig. 1 shows the different classification levels and subtasks of the aspect level of sentiment analysis.

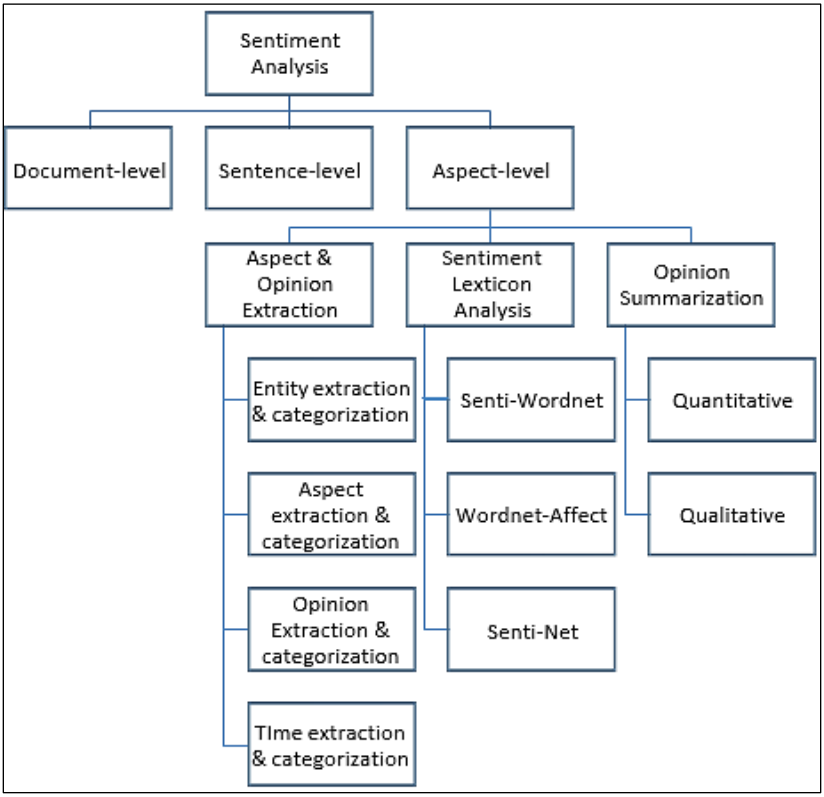

Fig 1: Classification of Sentiment Analysis

III. Feature selection and classification of sentiment analysis

This work discusses the sentiment analysis phase to identify sentiment-based circles with respect to various issues or events. The normalized and structured tweets in the form of unigrams in the pre-processing phase have been used to identify the sentiments of the tweets. In this work, a technique has been proposed to analyze the public sentiment by using a combination of Natural Language Processing techniques with supervised learning. First step, data pre-processing model is proposed to optimize the collected dataset and in further continuation as second step perform the experiments to analyze the machine learning methods to obtain the performance results. Second step helps for evaluating the performance vector for various schemes of feature selection and up to 4-grams (i.e. n=1, 2, 3, 4) in this work. The model for the proposed technique is depicted in Fig.2.

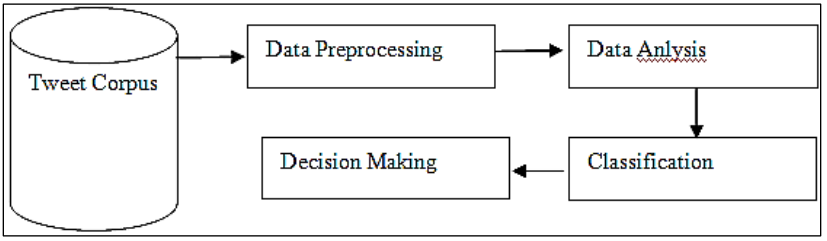

Fig 2: Framework of sentiment analysis

A model has been implemented by using Linear Support Vector Machine in RStudio. As first step pre-process the training datasets and then apply 5-fold cross-validation to train the linear support vector machine classifier. To test the performance and compare the results Naïve Bayes classifier feature selection technique is also used.

Data pre-processing

The general techniques for data collection from the web are loosely controlled and therefore the resultant datasets consist of irrelevant and duplication information. Dataset has been processed through many pre-processing steps to optimize it for further experimentations. The proposed model for data pre-processing is shown in Fig.3

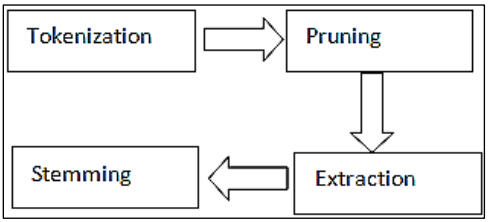

Fig 3: Data pre-processing Steps

Algorithm to create word vector from tweet corpus

- Input Tweet corpus T.
- Read tweets from corpus to generate new data set Tn.
- Design a token set D from dataset Tn.
- For each token ti in the dataset D do.

If(5<= ti <= 10000)/*10000 maximum number of documentsTj □ ti

Else

Discard token ti

- For each token tj in the new token set Tj do

If(5<= tj <= 10000)

Tk ⇓ tj

Else

Discard token tj

- Apply stemming algorithm to the new token set Tk

  Stemming Language (Tk) ⇓ Language

Data pre-processing steps

Tokenization

In this process text of the document has been split into tokens or unigrams for further processing. The splitting is done on the basis of finding space and non-letter characters found in the dataset. This process results the dataset into single word i.e. unigrams.

Pruning

The dataset has been pruned to remove the unnecessary frequently used words to remove the noisy text. Text has been processed on the basis of two parameters by keeping a value of below and above the pruning parameter. The text matching these two parameters has been used for further processing. The value of these parameters was set as: pruned below 5 and pruned above 10000 i.e. ignoring the words that appear in less than 5 documents and in more than 10000 documents.

Filtering tokens

Filter has been applied on the token set for decreasing the noise from dataset. The parameters used to filter out the tokens are the minimum length and maximum length. The parameters define the range for selecting the tokens. In the proposed model the minimum length was set to 4 characters and maximum length to 25 characters i.e. tokens having length less than 4 and greater than 25 characters has been removed as these will not play a vital role in the process.

Stemming

Stemming is a process to discarded extra ending characters and keeping the stem or root word in the dataset. After discarding the extra characters used in the end of words, dataset has been applied for stemming to decrease the length of words to match a minimum requirement. This process can be done with two main rules:

Trimming

The general rules for dropping the endings from words include:

i) If a word ending with "es" then character "s" can be discarded.

ii) If a word ending with consonant except "s", followed by "s" then s has beendiscarded.

iii) If a word is ending with "ing" and "ed" then word has been trimmed to get aproper English word.

Transforming the words

The words can be transformed to some other grammatical form using a set of defined rules. For example, if the word ends with "ies" but not "eies" and "aies" then the "ies" can be replaced with a "y" such as "Butterflies" can be replaced with "butterfly".

Table 1: Example of stemming

Word	Stem
Account, Accounts, accounting, accountant, accountable	Account
Used, user, users, using, usable	Use
Trust, trustworthy, trustable	Trust

The stemming technique increases the efficiency and effectiveness of the information retrieval and text mining processes. Matching the similar words results in improved recall rate and also reduces the indexing size as much as 40-50%.

Feature selection

This step generates a word vector which includes occurrence of a token, binary token occurrence and the frequency of term related to the document known as TF-IDF(Term Frequency-Inverse Document Frequency).

These are based on the following values:

1) $\mathbf{T_{xy}}$**:** Total number of existence of term x in document y.

2) $\mathbf{T_{dy}}$**:** Total number of terms existing in document y.

3) $\mathbf{T_{tx}}$**:** Total number of documents where term x occurs.

Term occurrence: defines the absolute number of occurrences of a term.

Term occurrence = T_{xy}

Term frequency: defines the relative frequency of a term in the document.

Term frequency = T_{xy}/T_{dy}

Binary term occurrence: term occurrence is defined as the binary value.Binary Term Occurrence = 1 for $T_{xy}>0$ and = 0 otherwise.

TF-IDF: it describes how important a word is for a document. It consists of two parts: term frequency (TF) and invert document frequency (IDF).

TF-IDF= $(T_{xy} /T_{dy})\log(1/T_{tx})$.

N-Grams

N-gram model shows the subtext of n terms in a given sequence of text. It is used in various fields of data analysis to find the correlation between the texts. This model shows the sequence of n-gram terms in a given document where value of n can vary like n=1 called unigrams, n=2 called bigrams and n=3 called trigram and so on. The value of n can be extended to find higher level of sequence of text. The n-gram model can be better explained with the following examples:

Text: "Demonetization is a good step of BJP."

Unigrams: "Demonetization", "is", "a", "good", "step", "of", "BJP".

Bigrams: "Demonetization is", "is a", "a good", "good step", "step of", "of BJP".

Trigrams: "Demonetization is a", "is a good", "a good step", "good step of", "step ofBJP".

Unigrams presents the simplest model for the n-gram approach by representing a single token where bigrams are the most frequently used two terms together in the whole document by combining the unigrams. The higher order grams can be formed in the similar way by taking together the n adjacent words. To find the context higher order n-grams are more useful because they provide the word position for better understanding.

Classification

In machine learning classification training dataset has been provided to train the classifier and for testing the performance test dataset has been given. It works like human beings where one can learn from their past experiences and predict the future decisions. These techniques are used for document classification and also in artificial intelligence. Machine learning classifier works in two steps:

1) Use dataset to train the model.

2) Use test dataset on the trained model to see the results and check accuracy of model.

In this work, Naïve Bayes and Support Vector Machine classifier have been used to analyse the dataset and then compare the results obtained from both of these techniques. With the help of these two techniques sentiment analysis task has been performed and then by comparing the results conclusion has been drawn.

NB (Naïve Bayes) classifier work on the basis of probability of the presence and absence of a term in the document, so this is a probabilistic classifier. This technique considers the independency of presence and absence of any feature corresponding to any other feature in a document. Naïve Bayes takes a document as a BOW (Bag of Words) and while calculating the probability of a word it does not consider the position of word within document and it related words i.e. presence or absence of other words related to this word. For a document d and class c:

Support vector machines have been the most efficient way for document classification as compared to Naïve Bayes and Maximum Entropy in almost all the cases. SVM works on the principle to separate a class within document by hyper plane with maximum margin from another class from the same document. This work initially considers Naïve Bayes classifier and the Linear Support Vector Machine for test the datasets. Later the linear support vector machine was used to train the model for obtaining the results for n-grams (n=1, 2, 3, 4). For experiment this model uses 100000 iterations to obtain the result.

IV. Results and Discussion

The dataset used for the experiments was divided into two classes, positive and negative. There are four possible outcomes for a given document in a classifier these can be true positive, true negative, false positive and false negative. If a document classified as negative and labelled as negative then it will comes under true negative otherwise it will be false negative. Same will be happen with the categorization of positive labelled dataset. Similarly, if a document is labelled negative and is classified as negative it is counted as true negative else if it is classified as positive it is counted as false positive. Based on these outcomes a two by two confusion matrix can be drawn for a given test set.

i) Accuracy = (tp+tn)/(P+N).

ii) Precision = tp/(tp+fp).

iii) Recall/true positive rate = tp/P.

iv) F-measure =2/((1/precision)+(1/recall)).

v) False alarm rate/false positive rate = fn/N.

vi) Specificity = tn/(fp+tn) = (1-fp rate).

The results shows that linear Support Vector Machine gives not that much accurate results as much accurate results given by term frequency inverse document frequency technique. Maximum accuracy is given for Naïve Bayes classifier and some good results are also shown by binary term occurrence in the text. After the variation in multiple parameters, Linear SVM perform better than Naïve Bayes. Total numbers of datasets are 2000 which are equally divided into positive andnegative i.e. 1000 each.

Conclusion

Many sentiment analysis methods rely on opinion lexicons as resources for evaluating the sentiment of a text passage. An opinion or sentiment lexicon is a dictionary of opinion words with their corresponding sentiment categories or semantic orientations. A semantic orientation is a numerical measure for representing the polarity and strength of words or expressions. Lexicons can be used to compute the polarity of a message by aggregating the orientation values of the opinion words it contains. They have also proven to be useful when used to extract features in supervised classification schemes.

References

1. Jansen BJ, Zhang M, Sobel K, Chowdury A. Micro-blogging as online word of mouth branding, CHI'09 Extended Abstracts on Human Factors in Computing Systems, Boston, MA, USA, 2009, 3859-3864.
2. Pang B, Lee L. Opinion mining and sentiment analysis, Foundations and trends in information retrieval. 2008; 2:1-135.
3. Bollen J, Mao H, Zeng X. Twitter mood predicts the stock market, Journal of Computational Science. 2011; 2:1-8.
4. Asur S, Huberman BA. Predicting the future with social media, Proc. of the 2010 IEEE/WIC/ACM International Conference on Web Intelligence and Intelligent Agent Technology, Washington, DC, USA: IEEE Computer Society. 2010; 1:492-499.
5. Avello DG. A meta-analysis of state-of-the-art electoral prediction from twitter data, Social Science Computer Review. 2010; 31:649-679.

6. Connor BO, Balasubramanyan R, Routledge BR, Smith NA. From Tweets to Polls: Linking Text Sentiment to Public Opinion Time Series, Proc. of the Fourth International AAAI Conference on Weblogs and Social Media, 2010, 122-129.
7. Pang B, Lee L, Vaithyanathan S. Thumbs up? sentiment classification using machine learning techniques, Proc. of the Conference on Empirical Methods on Natural Language Processing, 2002, 79-86.
8. Turney PD. Thumbs up or thumbs down? semantic orientation applied to unsupervised classification of reviews, Proc. of the Annual Meeting of the Association for Computational Linguistics, 2002, 417-424.

Chapter - 7
Intrusion Detection using Machine Learning Techniques

Authors

J. Anitha
Associate Professor, Department of CSE, Malla Reddy Engineering College (A), Hyderabad, Telangana, India

China Raju Manda
Assistant Professor, Department of ECE, JNTUK University College of Engineering, Vizianagaram, Andhra Pradesh, India

Suragala Ashok
Assistant Professor, Department of CSE, JNTUK University College of Engineering, Vizianagaram, Andhra Pradesh, India

Chapter - 7

Intrusion Detection using Machine Learning Techniques

J. Anitha, China Raju Manda and Suragala Ashok

Abstract

This work manifests detailed analysis of various classification models. The major categories of classification model include the Supervised and Unsupervised machine learning techniques. In supervised machine learning technique the training data is known and labeled over which a new instance is classified, whereas in the unsupervised machine learning, clustering mechanism is adopted to group the similar kind of objects and then they are classified accordingly. It provides an explanation about the types of classifiers such as single classifier, ensemble classifier and hybrid classifier, and also elaborates various feature selection techniques such as filter, wrapper and hybrid methods.

Keywords: machine learning, supervised learning, un-supervised learning

I. Introduction

An IDS supervises one single system or group of systems over a network for malevolent activities such as attacks over the system, larceny of the data or mischievous corruption of the network (Sommer and Paxson, 2010). In order to handle the detection activity without human intervention, machine learning approaches are used, which in turn will increase the detection rates, increase the quality of the detection thus lowering the false alarm with less computation overhead and also cost effective.

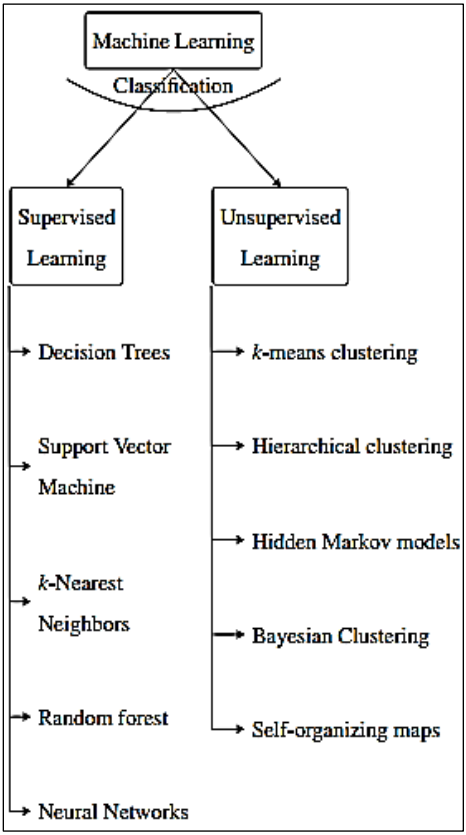

Fig 1: Machine Learning Techniques

Machine Learning techniques is broadly classified as Supervised machine learning technique, Unsupervised machine learning technique and Reinforcement machine learning technique. Supervised machine learning, where model is trained with training samples and new prediction is done over the prior knowledge. Unsupervised machine learning, where the model analyzes the data given and forms a mapping based on the properties of the data over the said constraints (Tsai *et al.*, 2009). Reinforcement machine learning, model develops itself with the reward and penalty process, and learns the environment based on the rewards. The thesis analyzes the Supervised and Unsupervised machine learning techniques for intrusion detection, as shown in Figure. 1.

II. Supervised machine learning

The supervised machine learning technique for intrusion detection endeavors to classify the normal and other categories based on the labeled

training instances (Fares *et al*., 2011). They have many benefits, as well as the aptitude of taking into account the inter- dependencies between variables and envisaging events, in addition to the capabilities of combining the prior knowledge and data. There exist various supervised learning algorithms like decision trees, support vector machines, *k*-nearest neighbor, random forest and neural networks for detecting anomaly (Belavagi and Muniyal, 2016).

III. Unsupervised Machine Learning

With the rapid advances in the network field, the type of attacks also parallelly keeps emerging, so along with the pattern matching and static techniques, the unsupervised learning techniques also contribute their comprehensive knowledge to detecting the attacks (Casas *et al*., 2012). Unsupervised learning deals with a set of samples that don't bear a labeling, so learning doesn't have any training over the labeled data-set, and as such unsupervised learning observes the data and figures out of a hidden structure from the data-set (Jiang *et al*., 2006), thus performing classification or clustering. Various unsupervised learning techniques such as *k*-means clustering, hierarchical clustering, hidden markov models, *k*-medoids and Self-Organizing Maps (SOM) are employed in IDSs (Tsai *et al*., 2009).

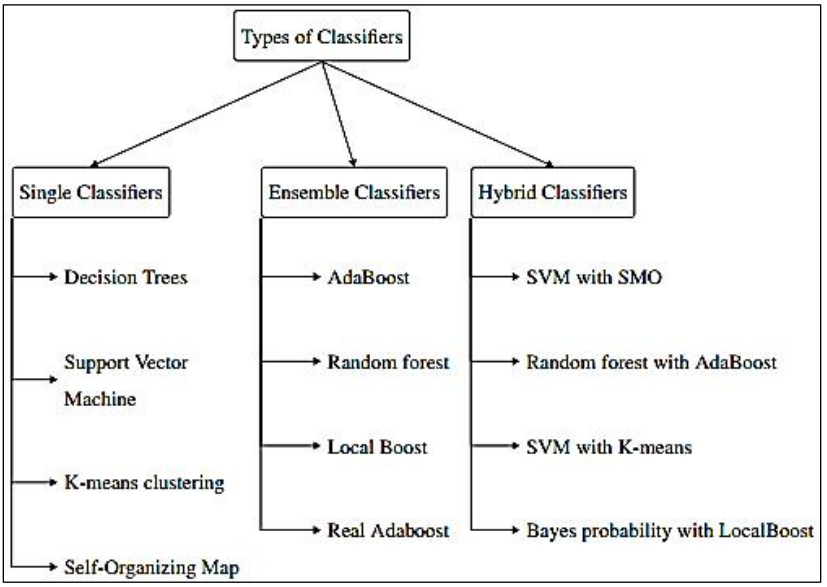

Fig 2: Types of Classifiers

This section describes briefly the various classifiers, its advantages, disadvantages and application over the IDS. Each classifier has a specific property and is used accordingly, but these classifiers may or may not be

associated with other classifiers in order to introduce varied forms of the classifier which may be a strong classifier or has been developed for a particular task. Those classifiers are further grouped into single, ensemble and hybrid classifiers (Sumana and Santhanam, 2014). Taken any classifier individually is studied as single classifier, the set of weak classifiers are grouped together to form strong classifier which is called as ensemble classifier and the classifiers cudgelled with the other one to overcome the pitfalls collectively are termed as hybrid classifiers. The Figure.2 displays the types of classifiers and few varieties of classifiers under each type.

Single classifiers

The single classifiers have broad domain over masteries such as clustering, prediction, regression and classification. This classification forms a set of heuristic rules to determine class or trains the model with the labeled data-set and predicts the unseen sample or studies the data and forms its own clusters thus enabling classification (Osadchy *et al*., 2016). Earlier methods of solving problems, where the human intervention was over the threshold and each instruction to the machine requires to be given as input, whereas the single classifiers were able to do jobs in an atomized way without much of human interference. These classifiers include SVMs, decision trees, *k*-means clustering and self-organized maps. But the limitation with these types of classifier is that it is unable to handle the realistic issues and possibly could provide misinterpretations.

Ensemble classifiers

The ensemble kind of classifiers combines the decisions of various weak classifiers together to form one strong classifier. Ensemble runs over a set of weak classifier repeatedly by distributing training data in order to accomplish a high detection rate. Ensemble is done by three ways: bagging, boosting and stacking (Rokach, 2010). The bagging works by decreasing the variance in the data-set, boosting uses the average working models together to increase the cost function, stacking works similar to boosting but instead of using the empirical weight function of the considered model uses another model for the estimation of weight. The ensemble type of classifiers include Adaboost, random forest, local boost and real Adaboost. The limitation with ensemble classifier is that it doesn’t produce best classification results on all datasets due to a poor choice of classifiers, and a simple classifier should be used as a base classifier in order to avoid over fitting issues.

Hybrid classifier

Hybrid classifiers use a set of heterogeneous methods, which are complimentary to each other, solving different tasks to accomplish one goal with the best classification accuracy (Olmeda and Ferna´ndez, 1997). Recent researches include a complicated set of data, and requires enhanced results and so it becomes a compulsion to include a combination of classifiers together to affect the accuracy rate. Hybridization can combine clustering, classification and association in any order to achieve the goals. Some of the hybrid approaches are SVM with SMO, Random forest with Adaboost, SVM with *k*-means clustering and Bayes probability with local boost (Gutta and Wechsler, 1997). If the whole describes the various Supervised and Unsupervised machine learning techniques to assist the known and unknown information for classification. Further it is beneficial to learn the dimensionality reduction techniques which play crucial role in the IDS.

Curse of dimensionality

Curse of dimensionality (Lee and Verleysen, 2007) is a fancy term coined to refer to a set of problems that arises with the expression of data using more dimensions than needed. It is instinctive to think that the fact of increasing the dimensions of data should not reduce the model's performance as actually the same amount or even more, information is provided. In such cases, the worst thing that can happen with added data is that the performance of the model should be same, but in practice, we find out that in most of the cases the performance actually decreases. The result is due to the limited training data that can be introduced to the system. In theory, the training data seems to be infinite and so the model ends up being perfectly trained under all the circumstances. In practice, this is impossible. The reason behind the curse of dimensionality is also known as empty space phenomenon given the sparse nature of high dimensional spaces. This sparsity is problematic for any method that requires statistical significance. The curse of dimensionality is better explained by Hughes Phenomenon, which states that "With fixed number of training samples, the predictive power reduces as the dimensionality increases". With the end goal to acquire statistically stable results the amount of data expected to help outcome increases exponentially with the added dimensions. Lots of problems arise due to curse of dimensionality. Some of them can be listed as follows:

- Wastage of storage space.
- Difficulty in visualizing the data at very high dimensions.
- Redundancy among the dimensions.

- Slowing down or the recognizer system.
- Sparsity of the data-set.

Feature selection

Feature Selection plays a prime role in intrusion detection. The motive of feature selection in intrusion detection is to acquire a set of features from the whole domain of feature set without hindering (Nguyen *et al*., 2010) the meaning of the information, and as well as maintaining positive effect on the classification accuracy. The feature selection embodies wrapper, filter and embedded methods (Stan´czyk, 2015).

Wrapper

The wrapper method of the feature selection forms a subset of principal features by verifying its utility in the classification. The enumerated predictive accuracy determines the relevance of the choice of the subset of features by an iterative process. As other methods, wrapper method also plays a fair task in identifying the fitting features for the problem (Kohavi and John, 1997). But the limitation with wrapper method with respect to intrusion detection is that the computation cost is comparatively high and if the training set is complex, the time complexity is also increased which makes its not feasible for the real-time applications like the IDS.

Filter

The filter model of feature selection identifies a sector of features which provides the highest predictive power. A statistical test is applied to the input values to determine which are more correlated to the specified output (Ambusaidi *et al*., 2016). Filter methods depend on the predictive task and data types. Filter methods broaden its domain into intrusion detection by identifying the outliers and find useful set of properties which will be capable of producing results of better accuracy.

Embedded

The Embedded model of feature selection unlike the filter and wrapper method, embodies the selection of features as part of the learning procedure itself, which are oriented towards the type of classification algorithm chosen. The advantage is that the computational time is less comparative to filter and wrapper methods but is specific to the considered machine learning technique. It is adaptable to IDS because the classifier, itself selects the features, as part of their learning, which may produce better accuracy and is very less prone to the over fitting issues (You *et al*., 2012).In general, in recent real-time applications, the dimensionality goes upto hundreds,

thousands to lakhs, which makes the existing feature selection techniques have quadratic or much higher time complexity to reduce the dimensionality and finds difficulty to scale up with higher dimensionality. The wrapper method works well if the training data is simple, when the complexity is increased then the time and computational entanglement parallelly increases, thus impeding the wrapper from real-time usage. The filter and embedded methods are more specific to the machine learning technique that is chosen for the issue, thus becoming mono-oriented to the technique used. Chen *et al*. (2006) survey over the various feature selection techniques and concludes that more improvisation should be done over the searching tactics and evaluation standards of selection techniques to convene with the increasing dimensionality of the data.

Conclusion

Various state of the art of machine learning techniques were discussed in this work. This work started with a brief introduction of each classification technique under Supervised and Unsupervised machine learning methodologies. Then we discussed the pros and cons of using the classifier as a single standalone or ensemble or as hybrid. Thereafter discussion over the importance of DR was given along with summary about curse of dimensionality. Consequently discourse about the categorization of dimension reduction into feature selection and feature extraction methods. The thesis work concentrates over the non-linear methods of feature extraction methodology.

References

1. Abbes T, Bouhoula A, Rusinowitch M. Efficient Decision Tree for Protocol Analysis in Intrusion Detection. International Journal of Security and Networks. 2010; 5(4):220-235.
2. Abduvaliyev A, Pathan ASK, Zhou J, Roman R, Wong WC. On the Vital areas of Intrusion Detection Systems in Wireless Sensor Networks. IEEE Communications Surveys & Tutorials. 2013; 15(3):1223-1237.
3. Abubakar AI, Chiroma H, Muaz SA, Ila LB. A Review of the Advances in Cyber Security Benchmark Datasets for Evaluating Data-driven based Intrusion Detection Systems. Procedia Computer Science. 2015; 62:221-227.
4. Aburomman AA, Reaz MBI. A novel SVM-kNN-PSO ensemble method for Intrusion Detection System. Applied Soft Computing. 2016a; 38:360-372.

5. Aburomman AA, Reaz MBI. Ensemble of Binary SVM classifiers based on PCA and LDA Feature Extraction for Intrusion Detection. In Proceedings of IEEE Advanced Information Management, Communicates, Electronic and Automation Control Conference, 2016b, 636-640.
6. Ahmed M, Mahmood AN, Hu J. A Survey of Network Anomaly Detection Techniques. Journal of Network and Computer Applications. 2016; 60:19-31.
7. Akhbardeh A, Jacobs MA. Comparative Analysis of Nonlinear Dimensionality Reduction Techniques for Breast MRI Segmentation. Medical Physics. 2012; 39(4):2275-2289.
8. Alarifi SS, Wolthusen SD. Detecting Anomalies in IaaS Environments through Virtual Machine Host System Call Analysis. In Proceedings of IEEE International Conference for Internet Technology and Secured Transactions, 2012, 211-218.
9. Almusallam NY, Tari Z, Bertok P, Zomaya AY. Dimensionality Reduction for Intrusion Detection Systems in Multi-data Streams-A Review and Proposal of Unsupervised Feature Selection Scheme. In Proceedings of Springer Emergent Computation, 2017, 467-487.
10. Amaral JP, Oliveira LM, Rodrigues JJ, Han G, Shu L. Policy and Network-based Intrusion Detection System for IPv6-enabled Wireless Sensor Networks. In Proceedings of IEEE International Conference on Communications, 2014, 1796-1801.